Flinders University

Design and Modelling Optimisation of VAWT-X Wind Turbine

By

Raphael Trinh

Thesis
Submitted to Flinders University
for the degree of

Master of Engineering (Mechanical)

College of Science and Engineering
22/05/2023

TABLE OF CONTENTS

ABSTRACT

Rapid reduction of greenhouse gas emissions is crucial in the fight against climate change. One of the most effective ways to achieve this is through the use of wind turbines. VAWT-X Energy is currently conducting research and development on their patented airfoil vertical axis wind turbines, which have the potential to be highly efficient when compared to horizontal axis wind turbines. A more efficient version of the helical-blade vertical axis wind turbine (VAWT) needs to be created and added to the current generator model owned by VAWT-X Energy. The proposed model considers the angles of the helical blades in the calculation, which allows for a clear demonstration of the differences in torque distribution between straight-bladed and helical-bladed VAWTs. It has been demonstrated that the torque on helical blades is evenly distributed, while there is a significant fluctuation of torque in the straight-blade VAWT. The VX-6/5 prototype and wind tunnel have been succesfully modified and constructed for the purpose of the experiment. The validation of the proposed model is heavily dependent on these pieces of equipment. The results of proposed model have been validated by comparing them with various VAWT models in the literature and achieving a good match in results. In addition, the good agreement also achieves while comparing with the experimental results collected from the VX-6/5 testing. The proposed model is successfully integrated with the current generator model, a strong agreement is reached through comparison with the parametric model developed by Lu and Zanj. The proposed model requires improvements to function at wind speeds below 3.5 m/s. Furthermore, it is possible to enhance both the wind quality and the experimental setup capacity by either incorporating additional components into the wind tunnel or upgrading to more powerful fans. Although It was demonstrated the new integrated parametric model is work with few testing parameters, more components and enhancement are required to further increase its modelling capacity..

DECLARATION

I certify that this thesis:

1. does not incorporate without acknowledgment any material previously submitted for a degree or diploma in any university
2. and the research within will not be submitted for any other future degree or diploma without the permission of Flinders University; and
3. to the best of my knowledge and belief, does not contain any material previously published or written by another person except where due reference is made in the text.

Removed due to copyright restriction

Signature of student.....

Print name of student.....Nguyen Binh Trinh.....

Date.....22/05/2023.....

I certify that I have read this thesis. In my opinion [redacted]/is not (please circle) fully adequate, in scope and in quality, as a thesis for the degree of Master of Mechanical Engineering. Furthermore, I confirm that I have provided feedback on this thesis and the student has implemented it minimally/partially/fully (please circle).

Removed due to copyright restriction

Signature of Principal Supervisor..... . .....

Print name of Principal Supervisor.....Amir.Zanj.....

Date.....22/05/2023.....

ACKNOWLEDGEMENTS

I am grateful for the support and guidance provided by Dr Amir Zanj, who is my supervisor during the course of this project. His mentorship has been invaluable in helping me to develop my skills and confidence as an engineer. I am grateful for the challenges he presented to me, as they motivated me to give my best effort.

I would like to express my gratitude to Mr Gary Andrews, who is a CEO of VAWT-X Energy. His agreement for me to join in this interesting and delightful project. As he works towards advancing his technology, I hope for his continued success in all his endeavours.

I would like to thank Mr Tim Hodge, who works as a Mechanical Support and Safety Compliance Officer and other staff in Engineering Services team. Their assistance in building the wind tunnel was invaluable and greatly appreciated.

I would like to express my gratitude to Brandon Lu for his innovative contributions to the original mathematical model and the excellent VX-6/5 prototype. Additionally, I am thankful to James Francis for his assistance in explaining the model and prototype components, and for providing me with valuable insights on this project.

Last but not least, I express my gratitude to my loved ones for their unwavering support that has propelled me to reach my full potential.

LIST OF FIGURES

LIST OF TABLES

NOMENCLATURE

Acronym	**Description**
BEM	Blade Element Momentum
DMST	Double Multiple Stream Tube
HAWT	Horizontal Axis Wind Turbine
MST	Multiple Stream Tube
PMSG	Permanent Magnet Synchronous Generator
rpm	Revolutions per minute
SST	Single Stream Tube
TSR	Tip speed ratio
VAWT	Vertical Axis Wind Turbine
Symbol	**Description**
A	Swept area
a_{dw}	Upstream Induction factor
a_{up}	Downstream Induction factor
c	Blade chord
C_d	Drag coefficient
C_l	Lift coefficient
C_n	Normal coefficient
C_p	Power coefficient
$C_{q_{av}}$	Average torque coefficient
C_t	Tangential coefficient
F_n	Normal component of resultant force
F_t	Tangential component of resultant force
H	Height of rotor
N	Number of blades
N_h	Number of Horizontal divisions
N_v	Number of Vertical divisions
Q	Aerodynamic torque
Q_{av}	Average aerodynamic torque
R	Radius of rotor
Re	Blade Reynolds number
V_{dw}	Downstream Induced velocity
V_{eq}	Equilibrium Induced velocity
V_r	Relative velocity

V_{up}	Upstream Induced velocity
V_{∞}	Freestream wind velocity

Greek Symbol	**Description**
α	Angle of attack
θ	azimuth angle
$\Delta\theta$	Individual azimuth angle
ΔF_n	Individual normal force
ΔF_t	Individual tangential force
Δh	Individual height of stream tube
ΔQ	Individual aerodynamic torque
λ	Tip speed ratio of turbine
$\Delta\lambda$	Individual tip speed ratio
ω	Angular velocity / Rotational speed
ρ	Air density
ν	Kinematic viscosity of air
Ψ	Helical angle

INTRODUCTION

Background Information

Governments and industries across the globe have made a significant commitment to reduce their greenhouse gas emissions to zero within the next two to three decades (IPCC 2022). In addition, a new report has found that governments worldwide can create millions of jobs, stimulate economic growth, and help achieve net-zero emissions by rapidly increasing the use of clean energy and reducing reliance on fossil fuels. This is the first comprehensive energy roadmap of its kind, showing that such actions are necessary and beneficial in multiple ways (IEA 2021). In short, to mitigate the effects of climate change, it is essential to decrease greenhouse gas emissions quickly; this is a difficult task that requires the development of more low-carbon technologies using renewable resources (Edenhofer 2014).

In the group of renewable resources, wind energy is a type of green energy that has experienced a considerable expansion in the past few years and is now one of the top sources of electricity worldwide (Global Wind Energy Council 2015). In 2022, the Department of Climate Change, Energy, the Environment and Water stated that wind, hydro and solar energy accounted for almost 30% of total electricity generation in Australia; this was the highest proportion of renewables in the history of Australia, surpassing the previous record of 26% in the mid-1960s (Energy.gov.au 2022).

Two types of wind turbines are used to generate electricity from wind energy: vertical axis wind turbines (VAWT) and horizontal axis wind turbines (HAWT). The former has a vertical axis, while the latter has a horizontal axis.

Figure 1 illustrates the configurations of these types of wind turbines, where HAWT is considered to be the most effective method to generate electricity (Ebrahimpour et al. 2019). Horizontal wind turbines come in two types: upwind and downwind. In upwind turbines, the rotor meets the wind direction, while in downwind turbines, the rotor is positioned behind the Nacelle. A yaw-controlling mechanism can also be installed in this type of wind turbine, which helps keep the rotational axis always parallel to the wind direction (Wang et al. 2019). However, the big drawback of HAWT is that it requires big landfill, part and installation costs. Meanwhile, VAWT is a cost-effective option for small-scale wind energy production,

particularly for residential use, because it requires less space for installation compared to the HAWT (Niranjana 2015).

VAWT **HAWT**

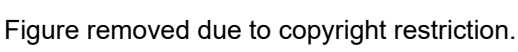

Figure 1 Diagrams of VAWT (Jiang et al. 2020) and HAWT (Bai & Wang 2016) configurations

In contrast to HAWT, VAWT has a rotational axis perpendicular to the wind direction. In addition, this type of turbine can generate electricity at low wind speeds. There are many types of VAWT, such as Darrieus, Savonius, H-blade and Gorlov have been found in the literature. VAWT is proven to be highly efficient in turbulent wind conditions, but it may not be practical for large-scale production purposes due to its complex blade aerodynamics (Nikam & Kherde 2015; Sun & Zhou 2022). Although VAWT is not commonly used for large-scale wind energy production, many VAWTs have still been constructed and employed for domestic purposes (Islam et al. 2008; Sharpe & Proven 2010; VAWT-X Energy 2022). VAWT technology has the potential to supplement current wind energy infrastructure and expand renewable energy production on a global scale with additional advancements (Solomin et al. 2020). Thus, this paper will present a more refined aerodynamic that enhances the performance and accuracy of the parametric model introduced by Lu and Zanj (2022).

Literature Review

Wind Turbine Modelling Methods

Throughout the history of wind turbine modelling, numerous researchers have used various modelling techniques to forecast the aerodynamic performance of VAWT. To determine the efficiency of a wind turbine, the power coefficient (C_p) of the rotor must be calculated. Several theoretical approaches employ Mathematics and Physics to progress research in this area. In the early stages, the most commonly used C_p prediction methods were based on momentum theory (Islam et al. 2008). It is widely recognised that these methods necessitate a significant amount of experimental data for drag coefficient (C_d), lift coefficient (C_l) and Reynolds numbers, covering a wide range of angles of attack (AOA). Researchers mostly used pre-selected algorithm (Zervos 1988) and one factor at a time (OFAAT) algorithm (Migliore & Fritschen 1982), incorporating the Momentum method.

Afterwards, the Panel method was utilised to estimate the coefficients of lift and drag of an airfoil. As a result, multiple programs based on this method were created to study the aerodynamic properties of airfoils (Somers & Maughmer 2003). However, the Panel method was only used by a small number of researchers to estimate the C_p of a Darrieus rotor (Wang et al. 2007; Dixon 2008); the Panel method is only able to handle mild separation because it does not account for the viscosity of the flow (Katz & Plotkin 2012).

Recently, the most sophisticated technique for observing the dynamic flow of liquids using computational software to employ the CFD method. This is because CFD can easily incorporate the dynamic stall, curvature and viscosity of flow effects into its analysis (Chen et al. 2016). Beri and Yao (2011a) used CFD to investigate the self-starting ability of two different airfoils. In 2012, Mohamed conducted his analysis using twenty chosen airfoils to predict the C_p of the Darrieus rotor on the CFD method (Castelli et al. 2012). Chen et al. (2016) conducted a study on the performance of a three-bladed H-type Darrieus VAWT using CFD analysis in both 2D and 3D simulations involving analysing the impact of various parameters of airfoil on the C_p. Furthermore, in a study by Subramanian et al. (2017), the researchers examined the impact of solidity ratio on CFD simulations and obtained simulated outcomes that were within 16% error when compared to experimental data from study of McLaren (2011). While CFD has demonstrated its capability to generate accurate results, it demands significant computational resources and is highly time-consuming, particularly in cases involving iterative design and optimisation processes. On the other

hand, if the airfoil characteristics are given, the Momentum method is quicker than both the Panel and CFD methods (Wang & Zhan 2013).

Blade Element Momentum Theory

Based on the general Momentum theory, Glauert (1935) developed a basic model for the ideal rotor that took into account the rotational velocity. This ideal rotor accelerates the flow in the axial direction by creating a pressure differential across rotor plane. In addition, this disk is considered to be a circular shape with an infinite number of blades (Bertram 2012).

The theory of actuator disks is based on the principles of Momentum, Conservation of Mass and Energy, and Bernoulli's equation. This concept was first introduced by Robert Edmund Froude in 1889 as a method to model the aerodynamics of flow in marine screw propellers, this theory was applied to turbomachines to simulate the axial flow through the cylindrical walls (Hawthorne & Horlock 1964). In other words, the Actuator Disk theory is a simplified version of the quasi-3D modelling, and It combines the 2D blade-to-blade cascade flow and the axisymmetric through flow (Gato & Falcao 2012). According to Lakshminarayana (1996), the process of solving the axial flow problem can be done efficiently using the streamline curvature throughflow method within the Actuator Disk theory. It was utilised to simulate the flow behaviour of the isolated rotor (Gato & Falcao 1988) and the rotor with guide vanes (Gato & Falcao 1990). Hence, the Actuator Disk theory is appropriate for analysing the flow patterns around the VAWT because it effectively simplifies 3D fluid dynamics problems into 2D problems.

The Blade Element theory was originally invented and published by Drzewiecki (1920), and it is an effective method for estimating the thrust produced by a rotor (39). The theory refers to a concept known as the blade element, which involves breaking a blade down into smaller elements. Each of these small elements is considered as a separate 2D airfoil. Furthermore, the calculation of aerodynamic forces is conducted by taking into account the conditions of the flow specific to each element. Ultimately, the aerodynamic properties of the entire rotor are determined by combining all of its smaller elements (Gudmundsson 2014). However, the simplified theory did not account for the induced flow within the rotor stream tube, resulting in the predicted thrust being greater than the actual thrust at the same conditions (Stepniewski 1979).

Blade Element Momentum theory, also known as BEM theory, is a well-known method that results from the combination of Blade Element theory and Momentum theory. In other words,

the Blade Element theory was advanced by Froude (1920) and Glauert (1935) via the utilisation of the momentum theory to represent the induced velocity within the stream tube. To summarise, the BEM theory serves as a fundamental basis for any additional principles or theories presented in this study.

Double Multiple Stream Tube (DMST)

The stream tube models were developed based on BEM theory. It is applied to determinie relative velocity of turbine blades and other aerodynamic properties of the turbine by studying the interaction between the turbine and fluid. By definition, a stream tube is formed by streamlines that make up its walls; this tube is impermeable, and no flow is perpendicular to these streamlines (Princeton University, n.d.). Single Stream Tube (SST) was invented by Templin (1974), and it introduced a single continuous stream tube which encloses the entire rotor. In this approach, the freestream velocity V_∞ was reduced to a constant induced velocity while the airflow passed through an actuator disk. However, this model does not take into consideration the variations between the turbine and fluid along the stream tube due to the constant velocity at the actuator disk. Wilson and Lissaman (1974) presented Multiple Stream Tube (MST) model to enhance the SST model, and this model divides the disk into multiple parallel stream tubes. In addition, The velocity generated in the MST model is calculated by the lift forces, which is determined using both the upstream and downstream regions. Furthermore, the MST was enhanced by incorporating the drag force on the blades into the momentum calculations (Strickland et al. 1979). Later on, Paraschivoiu (1982) presented Double Multiple Stream Tube (DMST) separating rotor into two regions: upstream and downstream. In the DMST model, each stream tube is studied as a combination of two actuator disks arranged one after the other. The air that flows through the downstream actuator is composed of the wake flow from the first actuator disk in the upstream region. The findings of this model have been shown to be in a close agreement with the experimental data (Paraschivoiu 1983). Figure 2 describes the differences between stream tube variations.

Single Streamtube Multiple Streamtube Double Multiple Streamtube

Figure 2 Variations of Stream Tube models (Adams & Chen 2017)

Gorlov VAWT Model

Professor Gorlov (1995) introduced the first Gorlov helical turbine, and this turbine was adapted from the straight blade Darrieus type to a helical blade design. While the turbine was initially created for water systems, it can also potentially be used in other renewable energy systems such as wind energy and wave energy. Furthermore, it has been demonstrated that the use of helical blades in the wind turbine design can reduce the torque instability that was present in the original straight blade design (Moghimi & Motawej 2020a). Some studies have used CFD simulations to investigate performance of helical blade VAWT. In a study of Alaimo et al. (2015), the aerodynamic performance of various straight and helical blade VAWTs, were conducted on 3D unsteady Reynolds-averaged Navier-Stokes simulation. As per their findings, the helical blade VAWT exhibits improved stability but generates lower power output. Moreover, Cheng et al. (2017) described the use of Large Eddy Simulation to simulate a 2D flow field of a four-bladed helical blade VAWT. The study investigated how tip speed ratio (TSR) changes affect the relationship between power output and variations in the azimuth angle. Two primary factors contribute to this correlation: blade-wake interaction and changes in angle of attack (AOA). Moghimi and Motawej (2020b) conducted a cost-effective model on MATLAB software for analysing the aerodynamic performance of the helical blade VAWT. The study examined how the aerodynamic performance and torque characteristics of the helical blade VAWT are affected by using several geometrical and operational parameters. In addition, the study involved analysing four distinct blade configurations belonging to the NACA symmetric airfoil family. According to their results, According to the results, the airfoil NACA0018 had the greatest C_p at a TSR of 3.5 (Moghimi & Motawej 2020b). Moreover, the results regarding TSR and C_p curve exhibit significant conformity when comparing with the experimental data of Quite Revolution 5 (Scheurich et al. 2010). Hence, the Gorlov VAWT model built in MATLAB shows the potential to accurately simulate the aerodynamic performance of the helical blade VAWT.

Case Study

History of VAWT-X Energy

VAWT-X Energy is a start-up company that is registered and based in South Australia. The company is focused on developing and certifying its patented airfoil for large scale production of two-bladed helical VAWTs. VAWT-X Energy specialises in producing wind turbines, including the VX-6, which has a power output of 6kW, and the VX-80, which has a power output of 80kW. Figure 3 describes the VX-6 prototype in the United Kingdom in 2013 (VAWT-X Energy 2022).

Figure 3 Previous prototype model of VX-6 turbine

VAWT-X Energy is working in close partnership with Flinders University to accelerate its products on research and development. As a result of collaboration, a MATLAB parametric model was invented to explore the performance of VX-6 turbine. Furthermore, a prototype called VX-6/5, which is a one-fifth scale version of the VX-6 turbine, was built at Flinders University. Recently, a wind tunnel has been built to conduct tests on the VX-6/5 prototype.

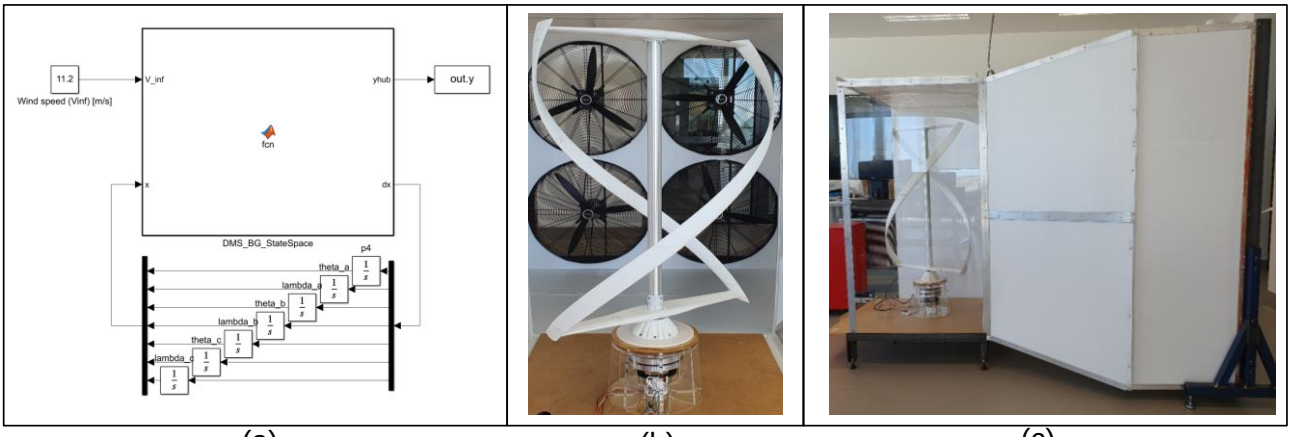

(a) (b) (c)

Figure 4 (a) MATLAB/Simulink Parametric Model; (b) VX-6/5 Prototype; (c) Wind Tunnel

MATLAB/Simulink Parametric Model of VAWT-X Energy

In 2022, Lu and Zanj developed a method for creating a multi-domain modelling platform for helical VAWT as shown in Figure 4a. The model requires multiple input parameters to determine various outputs. The model consists of two main parts aerodynamic model and generator model. The aerodynamic model was created by using MATLAB to simulate a straight blade VAWT and was based on BEM theory and DMST model. Also, the performance of a Permanent Magnet Synchronous Generator (PMSG) was modelled using Simulink graphical programming environment and the Bond Graph method. Finally, the data of a VX-6 turbine was used to validate the entire model. However, there are still some limitations exist in the model that might impact the result accuracy. The constant torque has been used along the blade in the MATLAB model to reduce the simulation time. As a result, the same properties are assumed in the entire blade, which is not possible in practice. Furthermore, due to the nature of the multi-domain modelling platform, there is still room for components extension to increase the feasibility of the software tool.

Experimental Setup

The experimental setup refers to the prototype, equipment and device that have been used for the purpose of testing and collecting data. The experimental setup consists of three main components: VX-6/5 Prototype, Wind Tunnel, Electronic equipment as seen in Figure 5.

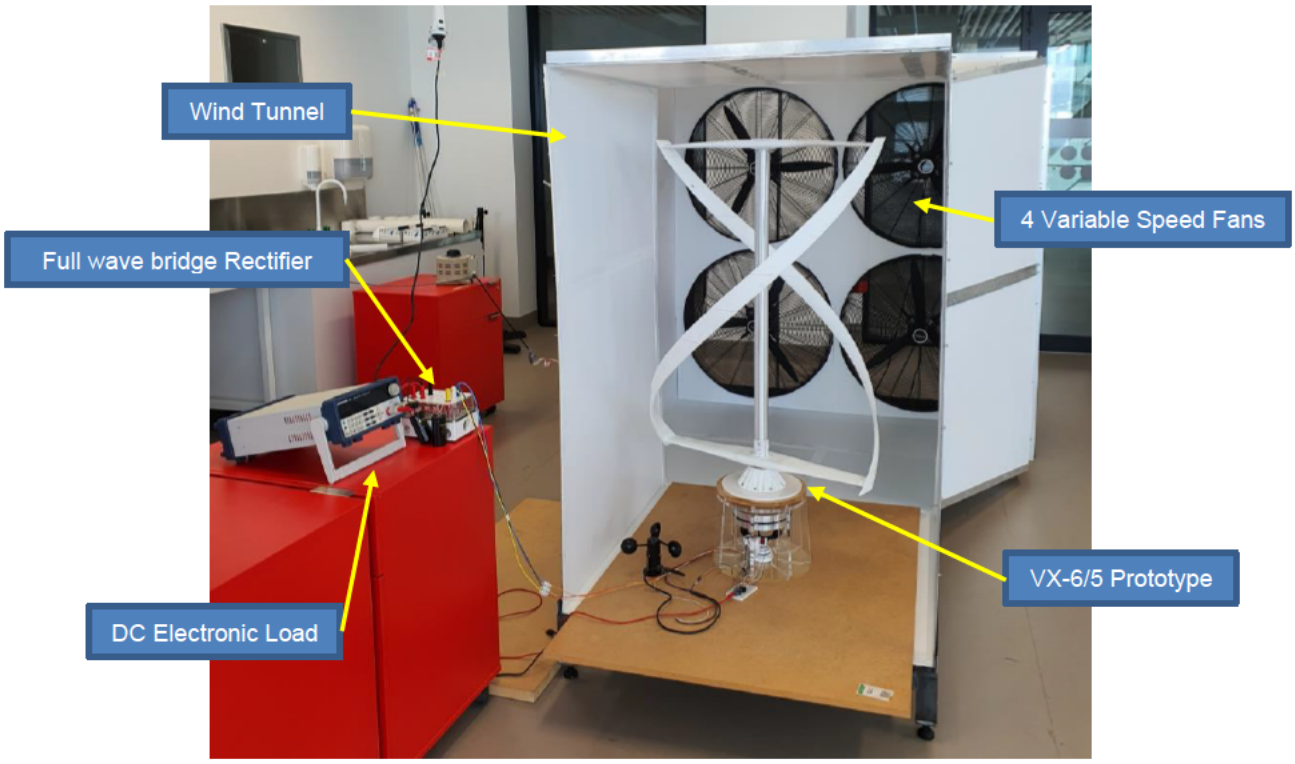

Figure 5 VX-6/5 Prototype and Wind Tunnel

VAWT-X Energy has constructed an approximate one-fifth scale of the VX-6 turbine, called the VX-6/5. The prototype was built in 2020. The prototype includes various sensors like an anemometer, a digital tachometer, and a load cell with an amplifier. In addition, electronic equipment such as an electronic load and a full wave bridge rectifier were set up to gather electrical signals during the experiments. The manager of VAWT-X Energy, Dr. Amir Zanj, has suggested that while the prototype has the ability to function as a testing protocol, further investigation and testing are required to confirm the validity of the parametric model. However, through several testings, the prototype has encountered numerous problems that required investigations and maintenances. One of the primary challenges encountered during the investigation was the difficulty in initiating the prototype, or self-starting issue. Therefore, it is crucial to conduct an investigation on this issue.

During the research period, the wind tunnel was constructed concurrently while conducting investigation on the VX-6/5 prototype. Even though the study did not originally involve wind tunnel testing, it was found to be important in improving the wind source to the VX-6/5 prototype as per supervisor suggestion. This helped address the self-starting issue of the VX-6/5 prototype.

Research Gap

Based on the literature review, it is evident that there is a significant lack of research on the helical-blade VAWT. Conducting research on this topic will not only benefit VAWT-X Energy, but also advance the understanding of helical-blade VAWT modelling.

As stated in the case study section, the current parametric model has limitations in accurately simulating the performance of a helical blade VAWT, as it was originally designed for a straight blade VAWT. The unsteadiness in the torque distribution of the straight blade VAWT model is caused by the sudden shifts in angle of attack. The helical geometry of the blade in the helical blade VAWT would minimise this effect. Furthermore, taking into account the angle of the helical blade can improve the precision of outcomes, albeit it might lead to a minor increase in the simulation duration. As a result, the Gorlov VAWT model has the potential to address these problems, making it a suitable approach for enhancing the parametric model of the VX-6 turbine.

Furthermore, the VX-6/5 prototype experiences self-starting issues that require additional investigation before the experimental setup can be reinstated. Upon the first examination of the VX-6/5 prototype, indications were found leading to modifying and upgrading processes

must be done such as bent vertical shaft and resistance during rotation. In addition, the testing environment was not optimal, as the prototype was situated in an exposed location, resulting in an unsteady and more turbulent wind source.

As a result, to optimise the model developed by Lu and Zanj (2022), there is a need that the Gorlov VAWT model must be investigated and integrated with the existing generator model. In addition, the experimental setup must also be investigated on the self-starting issue. Validation of the Gorlov vertical-axis wind turbine model against the performance of the VX-6/5 prototype is also required. Hence, it is necessary to address these gaps in order to enhance the effectiveness of VAWTs and facilitate their advancement and implementation.

Project Scope

The project aims to optimise and increase the capacity of the mathematical model and experimental setup of the VAWT-X wind turbines. According to Figure 6, this study has three main goals and several objectives that must be me. The first goal is to improve the current aerodynamic model by incorporating the new Gorlov VAWT model. The second goal is to modify and improve the current experimental setup to be ready for the validation stage. The third objective is to confirm the accuracy of the new Gorlov VAWT model by comparing its results with the current aerodynamic model, the experimental and other aerodynamic results found in the literature. Moreover, the new model should be able to combine with the generator model to form a complete system model.

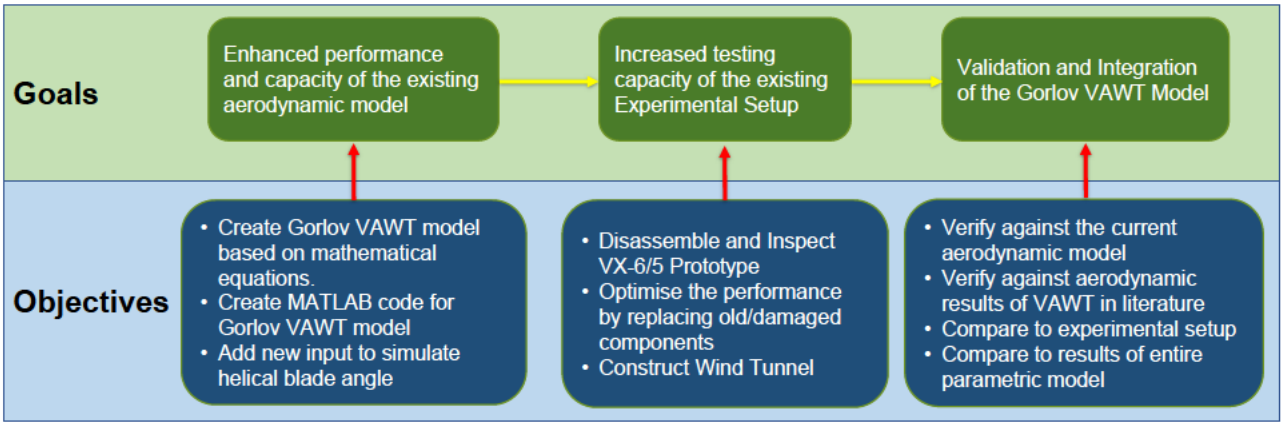

Figure 6 Project Goals and Objectives

As mentioned in the case study section, the parametric model is composed of an aerodynamic model and a generator model. This study aimed to optimise only the performance of the aerodynamic model, meaning that the generator model was beyond the scope of this project.

METHODOLOGY

Gorlov VAWT Modelling

The BEM theory is a combination of the Actuator Disc theory and Blade Element theory. Therefore, the following assumptions are critical while using these theories for wind turbine analysis, as shown in Table 1.

Table 1 Assumptions for analysis on BEM theory (Gudmundsson 2014; Burton et al. 2011; Beri & Yao 2011b)

No.	Assumptions
1.	2D Analysis and actuator disk is essentially a discontinuity moving through the fluid
2	Infinitesimally thin disk of area which offers no resistance to fluid passing through it as frictional forces are negligible compared with momentum flux and pressure changes
3	In the far-field regions, upstream and downstream of the actuator disk, the streamlines are parallel
4	Inviscid, incompressible, and isentropic flow
5	A control volume surrounds the stream tube and sharply separates the flow going through it from the surrounding air
6	The propellor does not impart rotation to the flow
7	The actuator disk is uniformly loaded and, therefore, experiences uniform flow passing through it.
8	No radial interaction between the flows through contiguous annuli

Formulas Derived from DMST Model

According to Parschivoiu (2002), two actuator disks are applied at the upstream and downstream regions of the rotor. Therefore, upstream and downstream induced velocities are determined at individual stream tube, as seen in Figure 7.

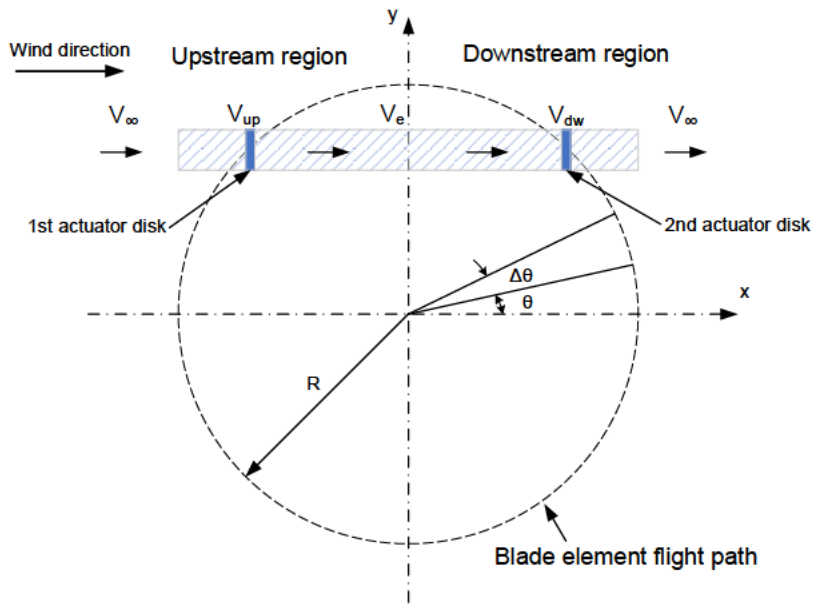

Figure 7 Top view of the rotor geometry for the Darrieus VAWT

By that, the free stream variations are considered in the analysis. By applying the conservation of mass and Bernoulli equation, the induced velocities are reduced in the direction of the flow as the wind flows through a stream tube. In other words, the upstream velocity (V_{up}) is less than upstream freestream velocity (V_{∞}), and downstream velocity (V_{dw}) is less than upstream velocity (V_{up}). In addition, in the middle section between upstream and downstream regions, equilibrium velocity (V_{eq}) exists, which value is smaller than upstream velocity (V_{up}), but higher than downstream velocity (V_{dw}).

$$V_{\infty} > V_{up} > V_{eq} > V_{dw}$$

In addition, the two induction factors at upstream and downstream regions are considered due to wind variations (Paraschivoiu 2002). These axial induction factors must be less than 1.

$$1 \; > \; a_{up} = \frac{V_{up}}{V_{\infty}} \; > \; a_{dw} = \frac{V_{dw}}{V_{eq}}$$

The above expression determines the induced velocities at upstream, downstream and equilibrium regions (Paraschivoiu 1981).

$$V_{up} = a_{up} V_{\infty} \qquad [1]$$

$$V_{eq} = (2a_{up} - 1) V_{\infty} \qquad [2]$$

$$V_{dw} = a_{dw}(2a_{up} - 1)\, V_{\infty} \quad [3]$$

The upstream induction factor (a_{up}) is assumed to be equal to 1 at the beginning. Hence, all induced velocities on the rotor blade have been found. The further calculations are broken down to calculate various parameters for both regions at each stream tube.

Upstream region calculations $(270^{\circ} < \theta < 90^{\circ})$

In order to determine the relative velocity and AOA acting on each element, the TSR must be defined based on angular velocity (ω), upstream velocity (V_{up}), and upstream AOA (a_{up}) (Kanyako & Janajreh 2014).

$$\Delta\lambda = \frac{\omega R}{V_{up}} \quad [4]$$

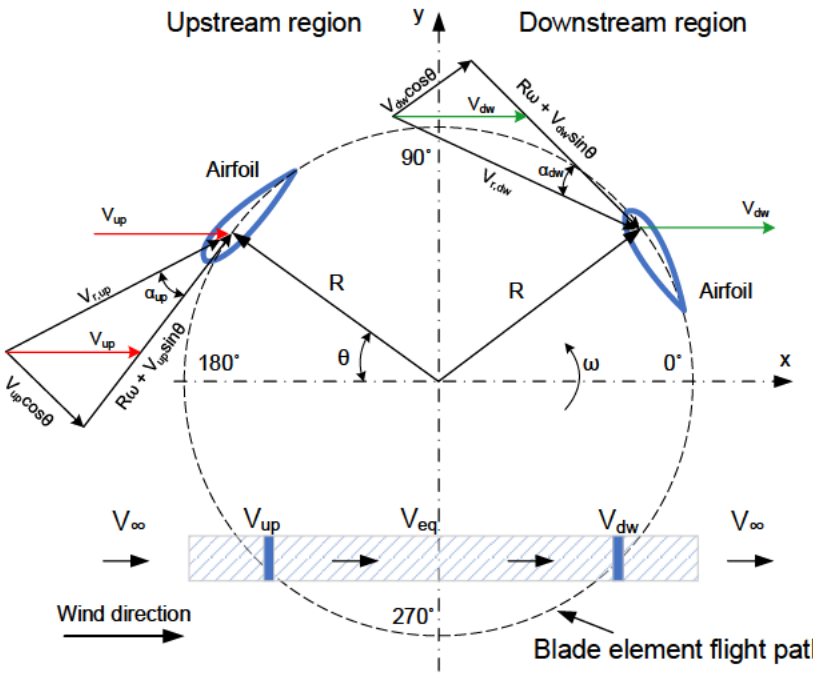

Figure 8 Relative velocity vectors at two regions of Darrieus VAWT

From Figure 8, the upstream relative velocity and upstream AOA are determined from trigonometry and simplified into the following equations (Saeidi et al. 2013).

$$\alpha_{up} = \tan^{-1}\left(\frac{a_{up}\cos(\theta)}{\Delta\lambda + a_{up}\sin(\theta)}\right) \quad [5]$$

$$V_{r_{up}} = V_{\infty}\sqrt{\left(\Delta\lambda + a_{up}\sin(\theta)\right)^2 + \left(a_{up}\cos(\theta)\right)^2} \quad [6]$$

According to (Meana-Fernández et al. 2018), the Reynolds number of turbine blade is the next parameter that needs to be calculated based on upstream relative velocity ($V_{r_{up}}$), blade chord (c), and kinematic viscosity (ν) of $1.461 \times 10^{-5}\ m^2/s$.

$$Re_{up} = \frac{V_{r_{up}} c}{\nu} \quad [7]$$

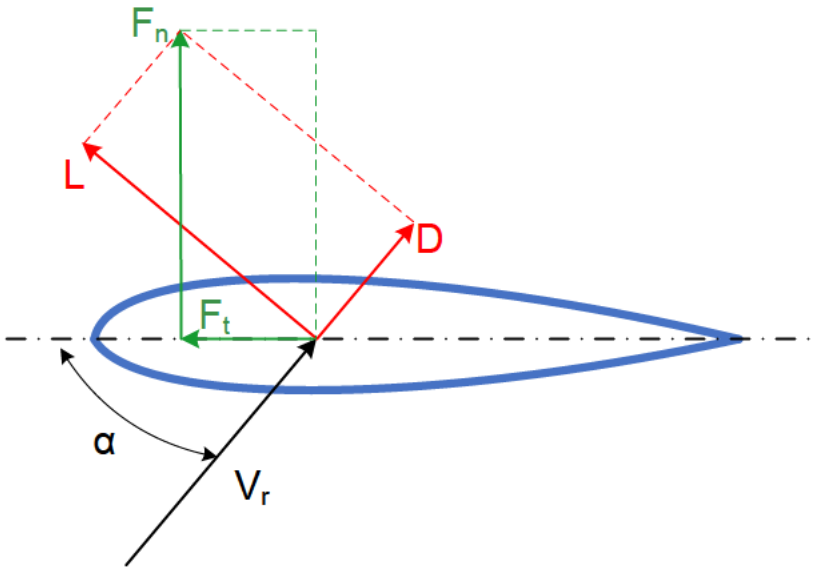

Figure 9 Aerodynamic forces loaded on wind turbine airfoil

Furthermore, normal coefficient (C_n) and tangential coefficient (C_t) need to be determined based on trigonometry, as seen in Figure 9. To do that, lift coefficient (C_l) and drag coefficient (C_d) must be known in advance. According to the experimental results of airfoil NAC0015 collected from AirfoilTools (n.d.) and QBlade software, the lift and drag coefficient series has been generated based on varying Reynolds number. The Reynolds number value has been varied between 0 and 5,000,000 to generate multiple sets of lift and drag coefficient results. The correct lift and drag coefficients are sorted and used for further calculations by interpolation. Hence, tangential and normal coefficients are found (Zhao et al. 2017).

$$C_t = C_l \sin(\alpha_{up}) - C_d \cos(\alpha_{up}) \quad [8]$$

$$C_n = C_l \cos(\alpha_{up}) + C_d \sin(\alpha_{up}) \quad [9]$$

It is required to calculate the new upstream induction factor, which can be compared with the initial induction factor in Equation 1. Paraschivoiu (2002) provided an upstream function that needed to be solved to calculate the new induction factor.

$$F_{up} = \frac{Nc}{8\pi R} \int_{\frac{3\pi}{2}}^{\frac{\pi}{2}} \left(\frac{V_{r_{up}}}{V_{up}}\right)^2 \left|\frac{1}{\cos(\theta)}\right| \left(C_n \cos(\theta) - C_t \sin(\theta)\right) d\theta \quad [10]$$

Hence, the new upstream induction factor is found as the following expression.

$$a_{up_{new}} = \frac{\pi}{F_{up}+\pi} \quad [11]$$

An iterative approach must be made for Equation 1 to 11. While comparing the new induction factor against the initial induction factor in each step, the residual of the subtraction between these two variables must be less than 0.0001 (Jafari et al. 2018).

$$a_{res} = a_{up_{new}} - a_{up} \quad [12]$$

The forces acting on each blade element of the VAWT, including aerodynamic torque (Svorcan et al. 2013), normal force and tangential force (Hashem & Mohamed 2017), can be calculated by taking into account geometrical factors such as the blade chord, rotor radius, rotor height, and air density of $1.225\ \mathrm{kg/m^3}$.

$$\Delta F_t = \frac{1}{2} V_{r_{up}}^2 C_t \rho c \Delta h \quad [13]$$

$$\Delta F_n = \frac{1}{2} V_{r_{up}}^2 C_n \rho c \Delta h \quad [14]$$

$$\Delta Q = \frac{1}{2} V_{r_{up}}^2 C_t \rho c R \Delta h \quad [15]$$

Downstream region calculations $(\mathbf{90^\circ < \theta < -90^\circ})$

The same parameters for the downstream region have been determined by following the same approach conducted in upstream region. A summary of all downstream region parameters is illustrated in Figure 10.

$$\Delta\lambda = \frac{\omega R}{V_{dw}} \quad [16]$$

$$V_{r_{dw}} = (2a_{up} - 1)V_\infty \sqrt{\left(\frac{\Delta\lambda}{(2a_{up} - 1)} + a_{dw}\sin(\theta)\right)^2 + (a_{dw}cos(\theta))^2} \quad [17]$$

$$\alpha_{dw} = \tan^{-1}\left(\frac{a_{dw}\cos(\theta)}{\frac{\Delta\lambda}{(2a_{up} - 1)} + a_{dw}\sin(\theta)}\right) \quad [18]$$

$$C_n = C_l \cos(\alpha_{dw}) + C_d \sin(\alpha_{dw}) \quad [19]$$

$$C_t = C_l \sin(\alpha_{dw}) - C_d \cos(\alpha_{dw}) \quad [20]$$

$$Re_{dw} = \frac{V_{r_{dw}} c}{\nu} \quad [21]$$

$$a_{dw} = \frac{\pi}{F_{dw} + \pi} \quad [22]$$

$$F_{dw} = \frac{Nc}{8\pi R}\int_{-\frac{\pi}{2}}^{\frac{\pi}{2}} \left(\frac{V_{r_{dw}}}{V_{dw}}\right)^2 \left|\frac{1}{\cos(\theta)}\right| (C_n\cos(\theta) - C_t\sin(\theta))d\theta \quad [23]$$

$$a_{res} = a_{dw_{new}} - a_{dw} \quad [24]$$

$$F_n = \frac{1}{2} V_{r_{dw}}^2 C_n \rho c \Delta h \quad [25]$$

$$F_t = \frac{1}{2} V_{r_{dw}}^2 C_t \rho c \Delta h \quad [26]$$

$$\Delta Q = \frac{1}{2} V_{r_{dw}}^2 C_t \rho c R \Delta h \quad [27]$$

Figure 10 Summary of downstream parameters

Simulating the helical blades of Gorlov VAWT

While applying the DMST model to wind turbine concepts, multiple small layers of the stream tube are arranged in a parallel manner, both horizontally and vertically. Induced velocities found in each layer of stream tube are distinct to each other due to varying individual azimuth angle ($\Delta\theta$) and individual height of stream tube (Δh), as shown in Figure 11.

Figure removed due to copyright restriction.

Figure 11 Diagram of multi-layered Gorlov VAWT (Moghimi & Motawej 2020b)

Horizontal layers (N_h) and can be determined by considering individual azimuth angle ($\Delta\theta$) and 180˚ degrees of the upstream region.

$$N_h = \frac{180°}{\Delta\theta}$$

For straight blade VAWT, the individual azimuth angle (Δh) can be simply replaced by the entire rotor height (H) because the forces and torque exerted at a specific azimuth angle are consistent throughout the rotor height. In contrast, the orientation of the blade in a helical blade VAWT is inclined along the height of the turbine. Consequently, it is vital to consider the angle of the helical blade in the DMST model to achieve the desired outcome. The relationship between the vertical layer (N_v) and helical angle (Ψ) can be determined from the following expressions.

$$N_v = \frac{\Psi}{\Delta\theta} \quad ; \quad \Delta h = \frac{H}{N_v}$$

Thus, the total torque generated by a single blade at a specific azimuth angle can be calculated using formulas that consider forces and torques produced in each horizontal and vertical layer.

$$Q = \sum_{1}^{2N_h} \sum_{1}^{N_v} \Delta Q \quad [28]$$

$$F_t = \sum_{1}^{2N_h} \sum_{1}^{N_v} \Delta F_t \quad [29]$$

$$F_n = \sum_{1}^{2N_h} \sum_{1}^{N_v} \Delta F_n \quad [30]$$

Furthermore, the total aerodynamic torque of the entire turbine and the value of torque coefficient are determined from the following equations.

$$Q_{av} = \frac{N}{2\pi} \int_{\frac{3\pi}{2}}^{-\frac{\pi}{2}} Q d\theta \quad [31]$$

$$C_{q_{av}} = \frac{Q_{av}}{\frac{1}{2}\rho A R V_\infty} \quad [32]$$

Ultimately, power coefficient of the Gorlov VAWT is determined by the following formulas.

$$\lambda = \frac{\omega R}{V_\infty} \quad [33]$$

$$C_p = \lambda \cdot C_{q_{av}} \quad [34]$$

Coding Algorithm of Gorlov VAWT Model

According to the formulas derived from the DMST model, a MATLAB code has been developed in order to predict the aerodynamic torque and power coefficient of the Gorlov VAWT. A flowchart describes coding algorithms for this section is shown in Figure 12.

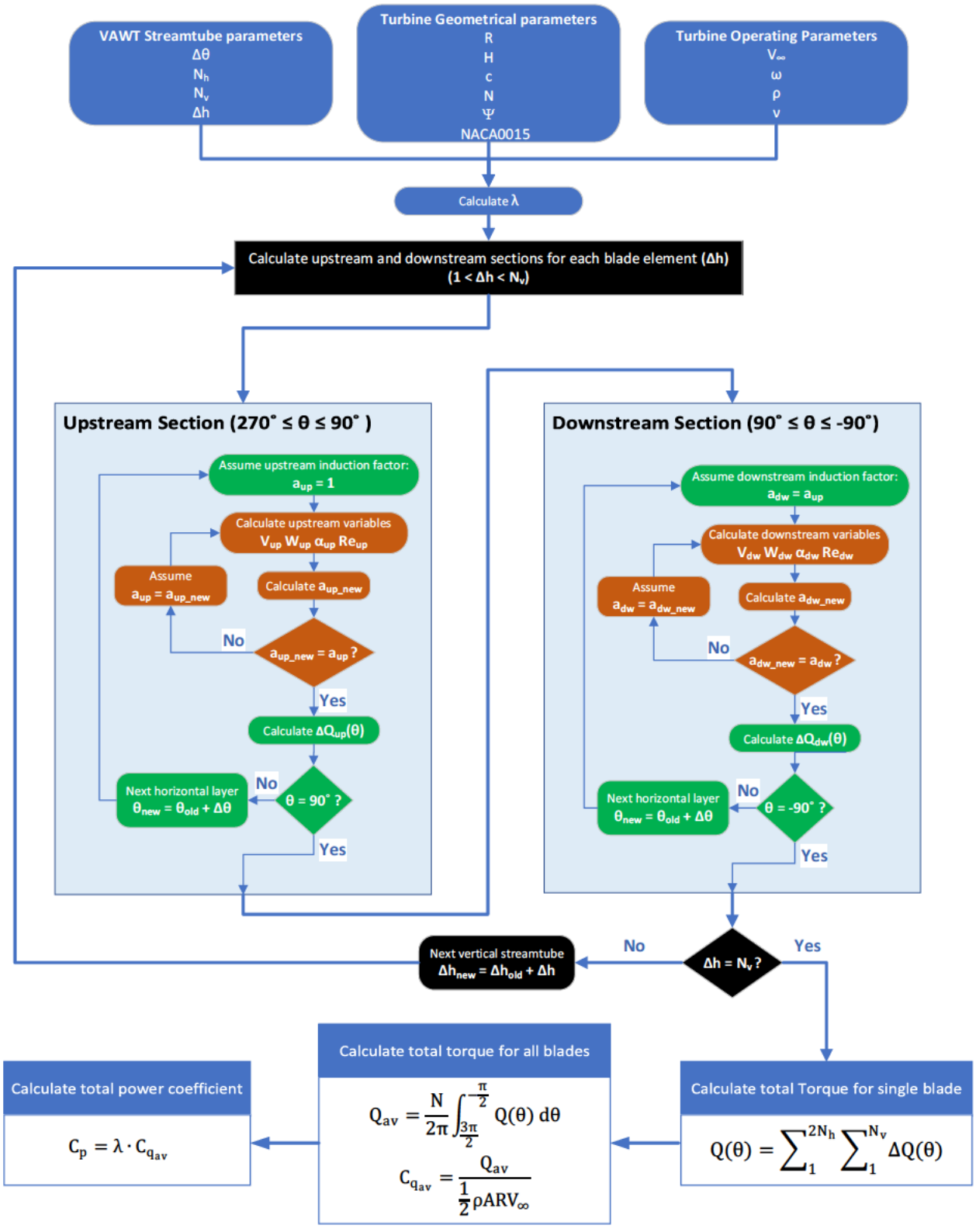

Figure 12 Flow chart of development of Gorlov VAWT in MATLAB

The system has three main predefined sets of input parameters. In the first set, the VAWT streamtube parameters include individual azimuth angle of blade, number of horizontal and vertical layers and helical angle of blade. In addition, the individual azimuth angle is a free variable and can be adjusted accordingly to ensure the accuracy of results. Simulations with smaller individual azimuth angles lead to more accurate results but take longer to run due to smaller blade elements being considered. The second set prescribes turbine geometrical parameters such as geometry of the VX-6 turbine and VX-6/5 prototype found in the Lu and Zanj study (2022), NACA0015 profile collected from AirfoilTools (2023) and QBlade software, and free parameter of helical angle is modifiable according to blade number and helical angle of blade. In this study, VX-6 turbine and VX-6/5 prototype is used for analysis which consists of two blades, and helical angle for each blade is 180˚. The third set consists of velocity of freestream wind, angular velocity of turbine, air density and kinematic viscosity. There are two free variables for the systems such as freestream wind velocity and angular velocity. Determining the initial TSR is a crucial step in the analysis process, and this requires the angular velocity to be predetermined.

Moreover, many iterations need to be conducted to determine forces and aerodynamic torques for each stream tube based on its horizontal and vertical layers. Furthermore, to determine the overall average aerodynamic torque of the turbine, the summation method is utilised to calculate the torque for each individual blade. This value is then multiplied by the number of blades and integrated over 360 degrees. At the end, torque coefficient and total power coefficient are calculated by using Equation 32 and Equation 34, respectively. The detail of MATLAB for the Gorlov VAWT model calculating aerodynamic properties of the VX-6 turbine and VX-6/5 prototype can be found in Appendix A.

Improvement in Experimental Setup

VX-6/5 Prototype Reinstatement and Upgrades

The experimental setup is crucial for testing and validating the aerodynamic or Gorlov VAWT model presented earlier. general, the experimental setup is an essential device for testing and validation against the aerodynamic model or Gorlov VAWT model proposed in the previous section. At the start of the study, it was discovered that the VX-6/5 prototype was not functioning due to a problem with self-starting. Despite receiving the full amount of wind energy generated from the fans, the prototype was unable to rotate, resulting in no collected outputs. As a result, the reinstatement plan has been proposed and many modifications and upgrades had been made upon to address the self-starting issue.

Initially, the disassembly plan has been produced to conduct a thorough analysis on its main components as seen in Figure 13.

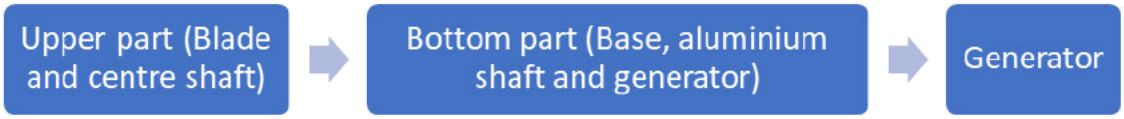

Figure 13 Disassembly plan of VX-6/5 prototype

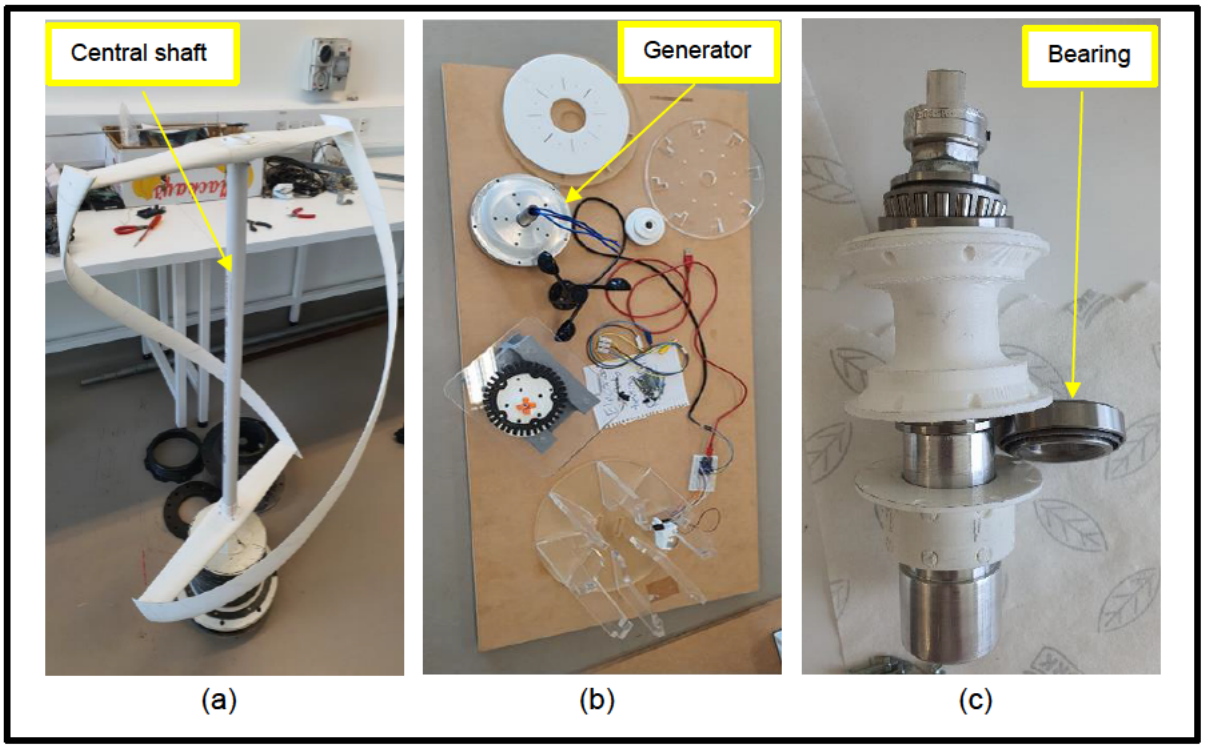

Figure 14 (a) Central shaft; (b) PMSG 12 poles generator; (c) Bearing

Based on the findings of the initial investigation as seen in Figure 14, the central shaft of the VX-6/5 was bent. In addition, the generator had problems with its rotating function, and one of two bearings used for the aluminium shaft at the bottom part was found to be damaged. Because of that, the corresponding solution for each problem has been delivered. The new aluminium central shaft has been manufactured with the same dimension of the previous plastic shaft. In addition, the generator has been disassembled by using Lathe Machine and found with many redundant glue and tapes attached on the inner components. The generator was able to function correctly after these redundant materials were removed. Moreover, the damaged bearing had been placed by the new bearing with same specification. Consequently, the assembly plan was followed, and the VX-6/5 was able to rotate smoothly, which is an important milestone for future testing of this prototype.

Wind Tunnel Fabrication

In order to improve the testing capabilities of the VX-6/5 prototype, the study recommends utilising a wind tunnel, which is an additional objective. The design of the wind tunnel is the property of VAWT-X Energy. The optimised design had been developed on Inventor software, taking into account manufacturing considerations that were not included in the original design. The wind tunnel has been fabricated following the optimised design, as shown in Figure 15. The primary objective of the wind tunnel is to improve the performance of VX-6/5 prototype, which aids in the validation process of the model.

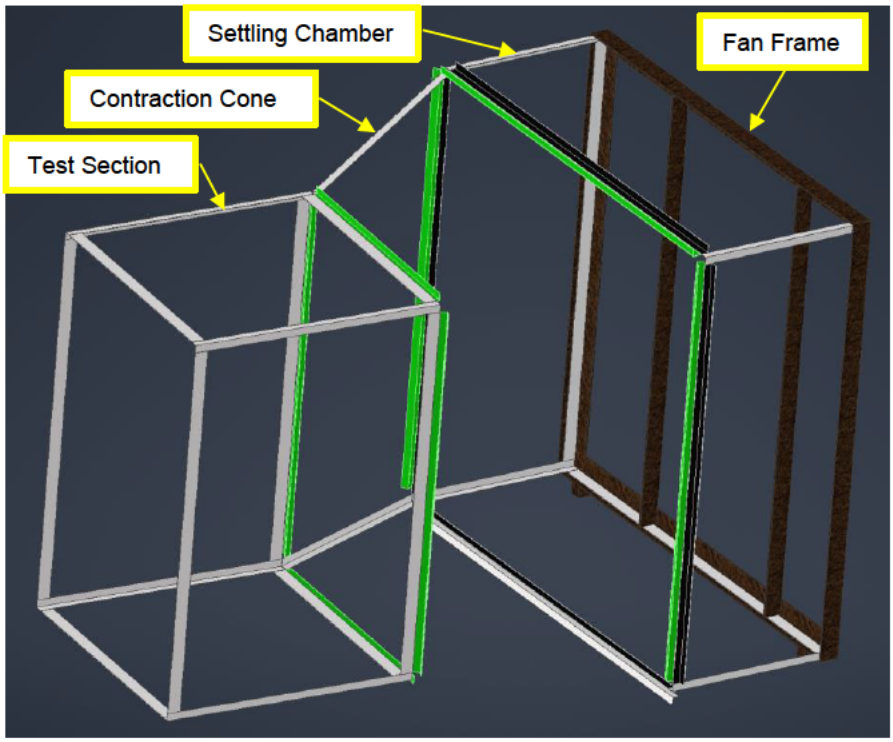

Figure 15 Optimised design of Wind Tunnel on Inventor

Validation Procedures

The validation stage is crucial to determine whether the proposed model is valid on general wind turbine technology and VAWT-X Energy turbines. The validation procedure consists of three main parts: a comparison of the results of Gorlov VAWT model against other models in the literature, against the results of the parametric model proposed by Lu and Zanj (2022), and against the experimental results of the VX-6/5 prototype.

Comparison on Aerodynamic Model

This section introduces the process of how the results are collected to validate on the aerodynamic performance of the Gorlov VAWT model. Results from Lu and Brandon (2022), Moghimi and Motawej (2020), and Paraschivoiu (2009) are used to compare against the results of Gorlov VAWT model. According to Figure 12, the input parameters are adjusted accordingly to different turbines and operational conditions. The primary objective of this section is to create various C_p vs TSR graphs for analysis.

Geometrical parameters

The results from different studies are collected based on different turbine geometry. Therefore, the parameters of R, H, c, N, and Ψ is be changed according to the turbines in each paper. Whereas the airfoil geometry is be set as NACA0015 for analysis. In addition, detailed information on geometrical parameters is be provided in the Results section.

Operational parameters

For operational parameters, the value of air density (ρ) and kinematic viscosity (ν) at 15˚C is constant at $1.225\,\mathrm{kg/m^3}$ and $1.461 \times 10^{-5}\,\mathrm{m^2/s}$ respectively (Engineering Toolbox 2003a; Engineering Toolbox 2003b). Additionally, the angular velocity (ω) is set according to each paper. Furthermore, the TSR is calculated using Equation 33, which includes three primary variables: angular velocity, rotor radius (R), and wind speed (V_∞). The values for angular velocity and rotor radius are fixed, while wind speed is varied between 1 and 30 m/s to produce the Cp vs TSR curves.

VAWT Streamtube parameters

In this group of parameters, the number of horizontal ($\mathrm{N_h}$) and vertical ($\mathrm{N_v}$) layers are affected by the individual azimuth angle ($\Delta\theta$), helical angle (Ψ) and turbine height (H). Helical angle and turbine height parameters are changed according to different papers. However, the individual azimuth angle is be set at 10˚ per stream tube. Tests were conducted with lower individual azimuth angles, which resulted in slightly more accurate results. However,

the simulation time was significantly longer. To speed up the simulation process for various wind speeds, it is useful to use an azimuth angle of 10 degrees for each individual test.

Comparison on Parametric Model

As previously mentioned in the Case Study section, the parametric model is comprised of an aerodynamic model and a generator model. The aerodynamic model has been optimized using the Gorlov VAWT model as suggested in the previous section. Meanwhile, the generator model, proposed by Lu & Zanj (2022), is remain unchanged. The generator model consists of several variables and state-space equations as referred to Appendix C. The equations were obtained by representing three-phase PSMG in Bond Graph system and then a MATLAB/Simulink coding algorithm was implemented according to Appendix C. The parametric model is built to investigate the performance of VAWT with respect to time. The main goal of this section is to combine the new aerodynamic model based on the Gorlov VAWT model with the generator model to form a complete parametric model as seen in Figure 16.

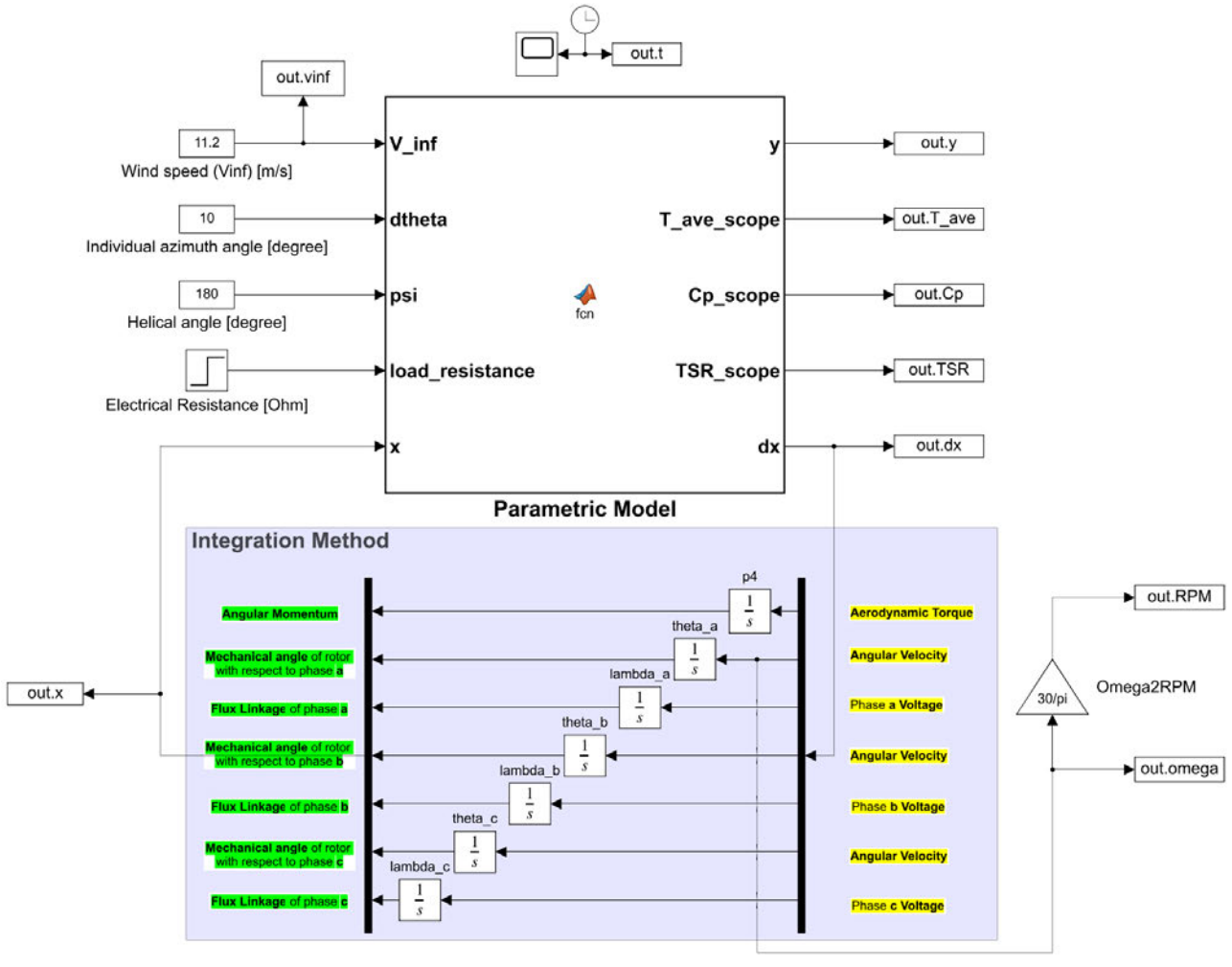

Figure 16 A complete parametric model in MATLAB/Simulink

Moreover, the parametric model in Figure 16 is be used to generate multiple aerodynamic outputs and electrical outputs. As a result, a comparison is made between the new parametric model and the existing parametric model proposed by Lu and Zanj (2022) to determine whether the new aerodynamic model can be integrated with the generator model.

Comparison on Experimental Setup

Experimental Equipment and Software

Figure 17 describes several required equipment that are used for the experiment. The VX-6/5 prototype has three sensors installed at located at the bottom of the turbine. Three sensors, an anemometer for measuring wind speed, a photo-interrupter tachometer for detecting angular velocity, and a load cell with an amplifier for calculating aerodynamic

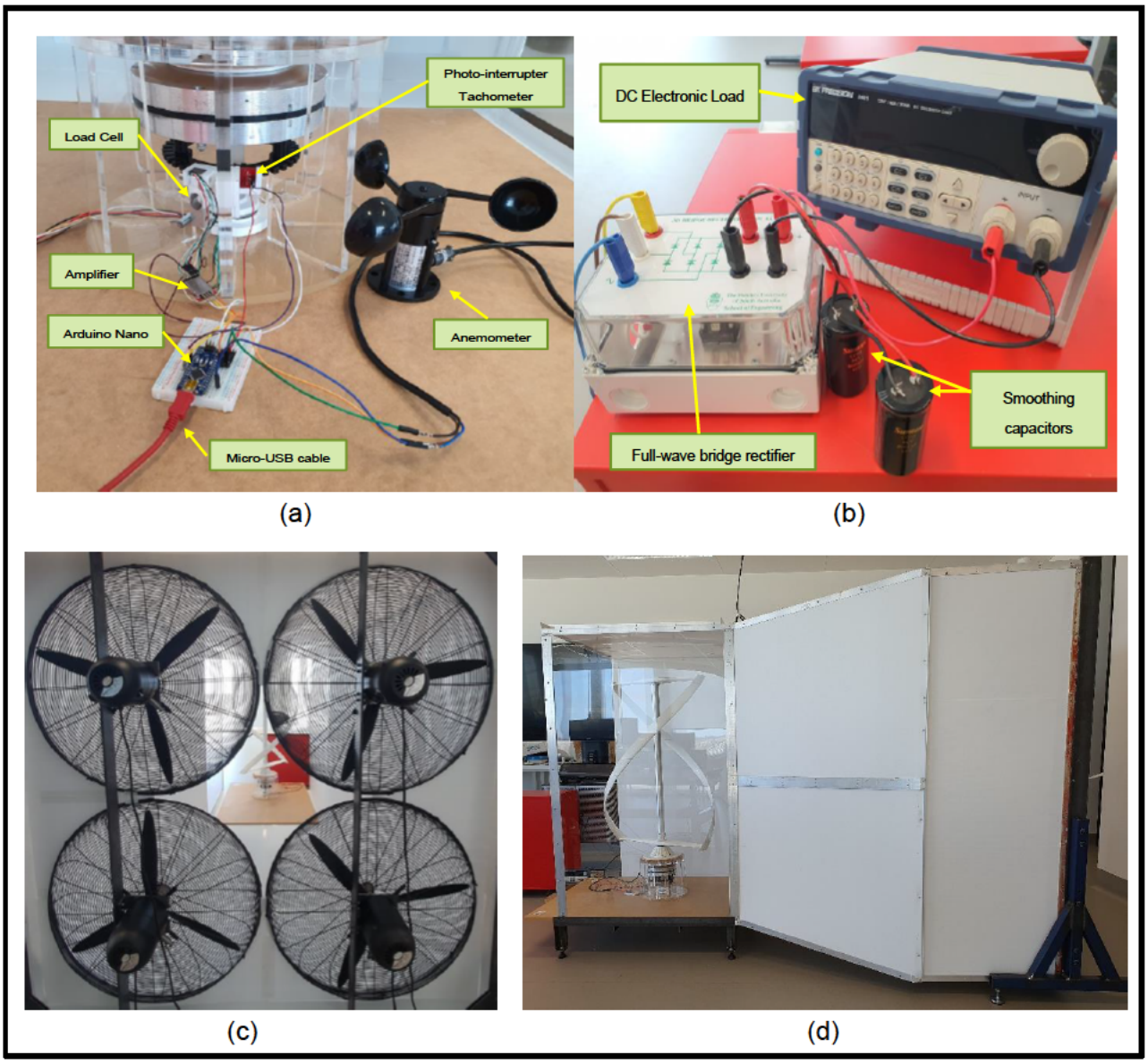

Figure 17 (a) Sensors installed in VX-6/5 prototye; (b) Electrical devices; (c) Wind-generated fan; (d) Wind tunnel

torque, are linked to an Arduino Nano microcontroller. Arduino and MATLAB codes for data collection has been provided by VAWT-X Energy manager. The sensor calibration has been completed beforehand and has been verified to accurately represent the actual results (Francis 2022). Figure 17b illustrates the electrical devices that have been connected to VX-6/5 prototype. The three-phase to DC bridge rectifier and two smoothing capacitors were developed by Lu (2021). Furthermore, the DC electronic load is used to regulate the electrical load, display electrical outputs for experimental data collection. Moreover, the four fans represent the incoming wind condition, and wind tunnel is used for enhancing the wind quality, as shown in Figure 17c-d.

Experimental Testing Procedure

In order to collect meaningful experimental results, it is necessary to follow the testing procedure depicted in Figure 18. The experiment started with the preparation of necessary hardware and software such as laptop, sensors, electronic devices, MATLAB software, Arduino software and Microsoft Excel. The prototype was found to only produce very small electrical voltage. When the electrical load was set to its maximum value of 7500 Ohms, the current reading could not be displayed on the electronic load due to its extremely low value. Therefore, an electrical load of 100 Ohms was used to obtain meaningful results.

At the beginning, the turbine must be started from rest for each test. In addition, various fan configurations were tested to determine the maximum number of fans that could turn the prototype at full speed. It is found that the turbine requires at least three fans in order to rotate. Therefore, the 3-fan and 4-fan settings had been used for this experiment. Following that, the wind speed was altered by adjusting the fan speed in each setting. The purpose of this is to vary the wind velocity, which is a significant factor in computing the TSR value according to Equation 33. In contrast to the Gorlov VAWT model, the angular velocity of VX-6/5 is adjusted based on the wind velocity during the experiment. Afterwards, a comparison was conducted to determine which configuration would enable the prototype to achieve the highest possible speed and electrical output. Ultimately, the optimal results were compared with those of the mathematical model during the validation phase.

Moreover, it is necessary to modify the mathematical model used in conjunction with the experimental setup to account for the characteristics of the VX-6/5. Furthermore, the input parameters, including wind velocity and angular velocity, must be adjusted based on the experimental results collected. For instance, the wind speed and angular velocity data

collected by sensors at fan speed level 3 should be inputted into the mathematical model to generate desired outputs for validation stage.

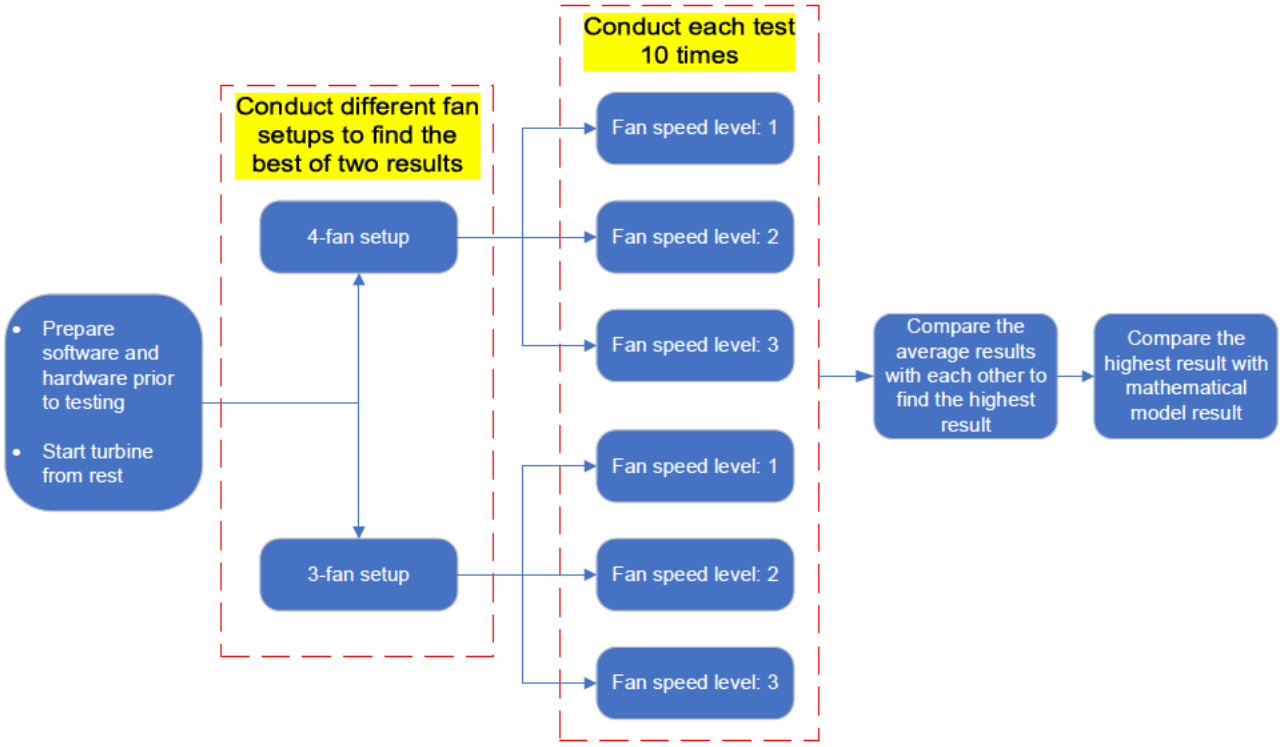

Figure 18 Experimental testing procedure of the VX-6/5 prototype

RESULTS

This section will present the findings of the study. It will begin by presenting the results obtained from the Gorlov VAWT model while comparing them with the results from other papers. Next, the Gorlov VAWT model will be combined with the generator model, and the results from the new parametric model will be compared with the previous parametric model developed by Lu and Zanj (2022). Lastly, the experimental results will be presented and compared to the results from the Gorlov VAWT model. Throughout this results section, the 'current model' term will used to refer to the result generated from the Gorlov VAWT model proposed in this study.

Comparison on Aerodynamic Model

Results Compared with Lu and Zanj (2022) study

Firstly, the results of Gorlov VAWT are compared against the results obtained from Lu and Zanj study (2022). Parameters shown in Table 2 are used with the MATLAB code provided in the Appendix A.

Table 2 VAWT characteristics in paper of Lu and Zanj (2022)

Parameter	Value	Unit
R	1.5	m
H	5	m
c	0.1875	m
N	2	
Ψ	180	degree
ω	260	rpm

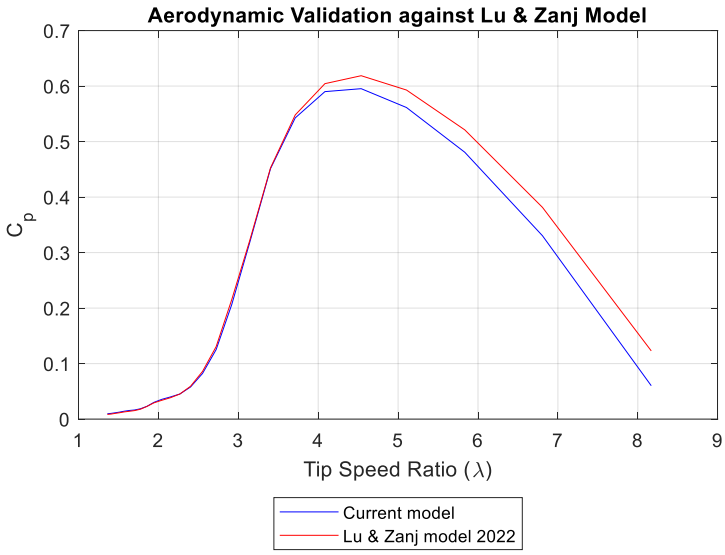

Figure 19 Validation of the current model with results from turbines presented in Lu and Zanj (2022) paper

The results from the current model are plotted together with those from Lu and Zanj (2022) and presented in Figure 19. The results show that there was a strong agreement between the two models under TSR of 3.7. Subsequently, the C_p result of the present model was lower than that of the other model. Moreover, both the current model and the Lu and Zanj model achieved their highest Cp values of 0.59 and 0.62, respectively, at a 4.5 TSR. The current model shows the range of TSR is between 1.3 to 8.2, and the Cp values vary from slightly above 0 to 0.59.

Difference in Torque Distribution

Figure 20 illustrates the torque exerted on the turbine throughout 360˚ rotation. In general, the results of upstream region (from -90˚ to 90˚) are higher than results in the downstream region (from 90˚ to the next -90˚). While the Cp vs TSR results are quite similar, the torque distribution results from the two models are significantly different. According to the current model, there is a slight fluctuation in aerodynamic torque. However, Lu and Zanj model shows a significant difference in the results. Maximum and minimum aerodynamic torque are 160 N.m at 30˚ azimuth angle and 115 N.m at 90˚ azimuth angle. The same pattern is seen in Lu and Zanj model, where the maximum torque of 295 N.m at 30˚, and minimum torque at 85˚ was a negative value. Consequently, the current model distributes the torque more uniformly throughout its rotation.

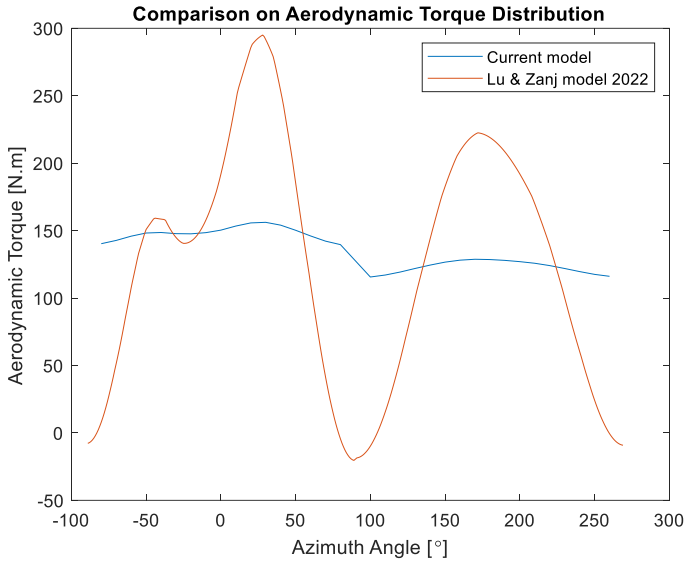

Figure 20 Torque distribution during a full revolution of VAWT

Results Compared with Moghimi and Motawej (2020) study

In Table 3, the three-bladed VAWT is used in this comparison. Hence, the helical angle is adjusted from 180˚ to 120˚. In addition, the angular velocity used in this analysis and the angular velocity used in the analysis is half of what was used in Lu and Zanj's model. According to Figure 21, the maximum C_p in two models is much smaller compared to what obtained in the previous case. The current model shows a maximum Cp of 0.49 at a 3.6 TSR, but Cp is low below a 2.5 TSR. Similarly, Moghimi and Matawej (2020) discovered that the maximum Cp value, which is 0.48, occurred at a TSR of 3.85. Additionally, the limited operating range is also defined by the TSR range of 0.5 to 6.5. Although the two models are in good agreement, the current model was discovered to have slightly superior performance when compared to the Moghimi and Motawej model.

Table 3 VAWT characteristics in paper of Moghimi and Motawej (2022)

Parameter	Value	Unit
R	1.5	m
H	5	m
c	0.2	m
N	3	
Ψ	120	degree
ω	125	rpm

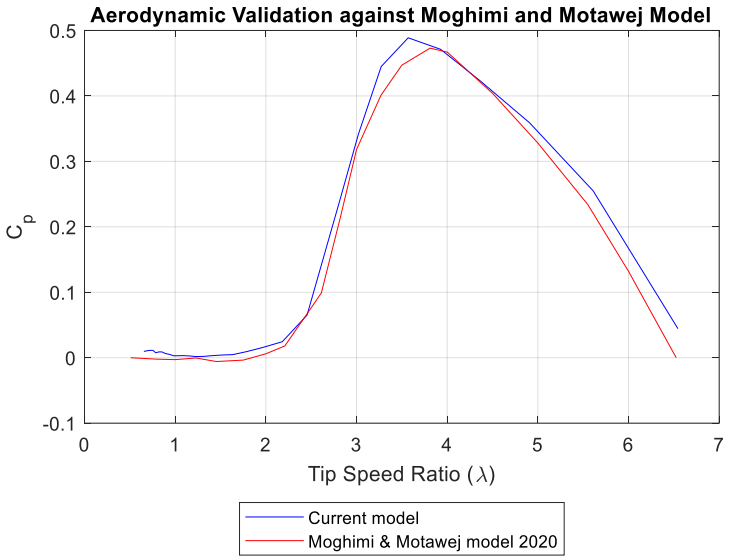

Figure 21 Validation of the current model with results from turbines presented in Moghimi and Motawej (2022) paper

Results Compared with Paraschivoiu (2009) study

In Figure 22, the Cp vs TSR curves is shown based on the parameters in Table 4. The results of two models are similar when TSR is below 4.3. However, when TSR exceeds 4.3, the current model outperforms Paraschivoiu's (2009) model. This VAWT has a high operational range than the previous two VAWTs, with TSR ranging from 0.3 to 9.8. In the current model, the highest Cp is observed at a TSR of 5.6, with a value of 0.48. In contrast, the Paraschivoiu model has a value of 0.45 at a TSR of 4.9.

Table 4 VAWT characteristics in paper of Paraschivoiu (2009)

Parameter	Value	Unit
R	3	m
H	6	m
c	0.2	m
N	2	
Ψ	180	degree
ω	125	rpm

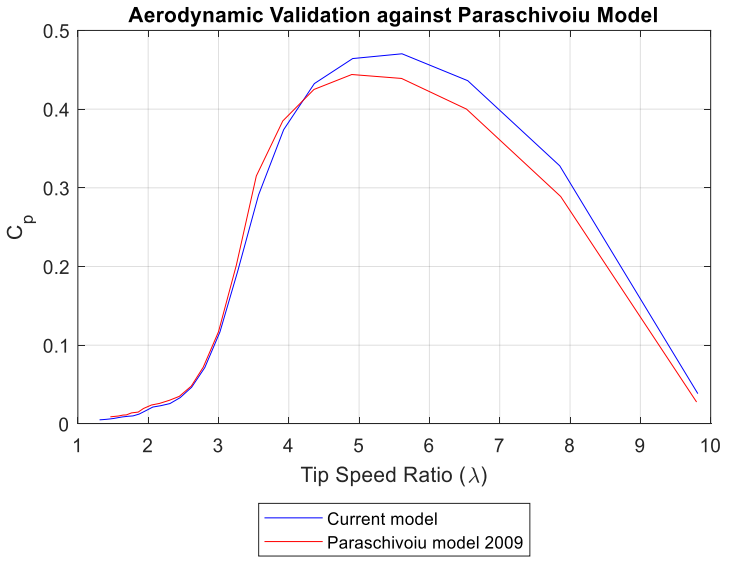

Figure 22 Validation of the current model with results from turbines presented in Paraschivoiu (2009) paper

Comparison on Parametric Model

The results in this section are mainly generated based on the parametric model displayed in Figure 16 and parameter table in Appendix C2. In addition, the code in Appendix A is combined with code in Appendix C3, then integrated in the function box in Simulink as seen in Figure 16. The parametric model was originally developed by Lu and Zanj (2022), then it was optimised by removing code redundancies in this study to slightly improve performance and reduce simulation time.

This section presents the various outcomes possible from the parametric model, including aerodynamic results and electrical outputs. The iterative approach permits the model to produce outputs continuously. It then generates new state variables by integrating results of state-space equations using the method outlined in Appendix C1.

Aerodynamic Outputs Comparison

Results were obtained after running the simulation for 5 seconds simulation time, but it took more than a minute due to many iterations. Several results such as C_p, TSR, aerodynamic torque, and angular velocity are generated in this section. the most important output is C_p vs TSR curve as shown in Figure 23. After running for 5 seconds, the Cp increases as the TSR increases. Both models produce outputs that are slightly different but essentially the same. At the end of the simulation, the highest Cp of 0.598 in current model and 0.6 in Lu and Zanj model (2022) at steady state as shown in Figure 24.

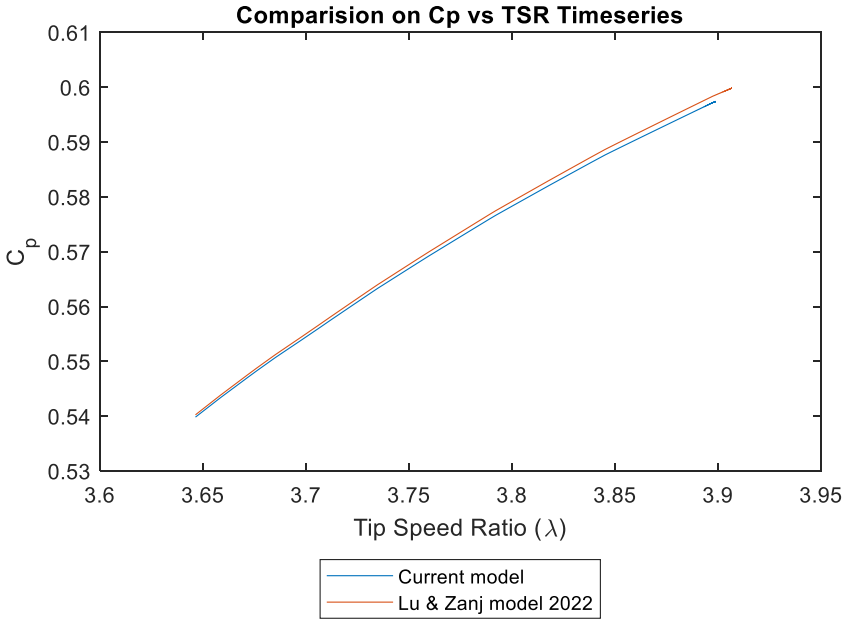

Figure 23 C_p vs TSR curve during 5 second simulation time

According to Figure 24, the outputs are increased at the start of the simulation. After 2 seconds, all results reached its steady state value. The initial values were produced using the code provided in Appendix A, and then increased while implementing state-space equations of the generator model, which are illustrated in Appendix C. All results generated from current model slightly lower than the results obtained from Lu & Zanj paper. This can be attributed to the fact that the Gorlov VAWT model generates less torque, resulting in lower values for other outputs. Based on these results, it can be concluded that the new model can be incorporated into the generator model, due to strong agreement of two models.

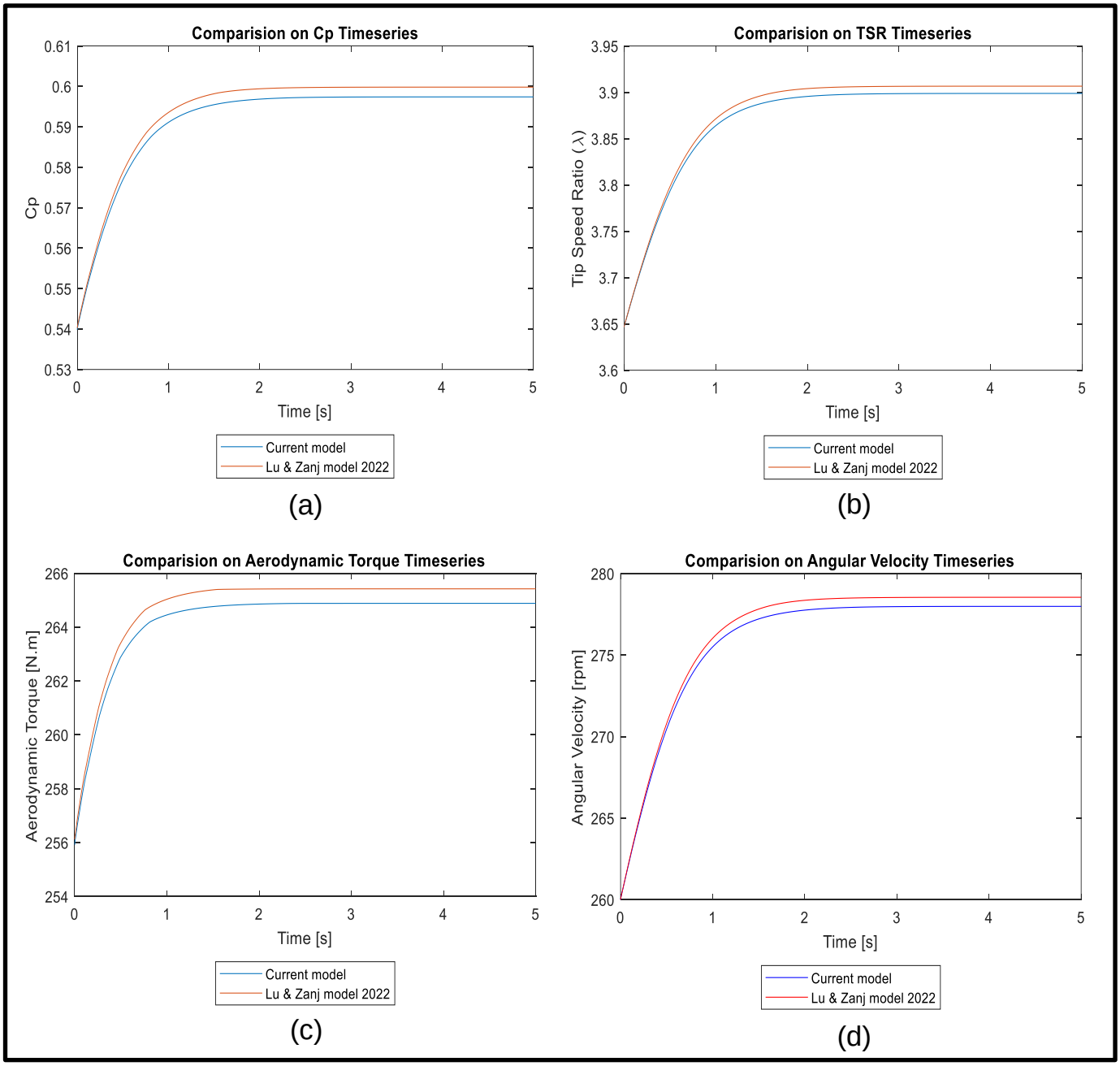

Figure 24 Aerodynamic outputs from parametric model
(a) C_p; (b) TSR; (c) Aerodynamic Torque; (d) Angular velocity

DC Electrical Outputs Comparison

The parametric model produces three-phase electrical outputs, which are obtained using state-space equations described in Appendix C2. Specifically, the voltage for each phase can be represented by the time derivative of certain variables, such as $\frac{dx_3}{dt}$, $\frac{dx_5}{dt}$, and $\frac{dx_7}{dt}$. Therefore, the current and power are determined according to the following equations:

$$I = \frac{V}{R} \quad ; \quad P = I \times R^2$$

From above equation, R equals to 21.3725 Ohm which can be found in table of parameter in Appendix C2. Therefore, the results of all electrical outputs are presented in Figure 25. To compare with the results from Lu and Zanj, it is necessary to determine the average values for each electrical output. The average values are obtained by taking the average of the peak and trough values at steady state. The steady state is achieved after running the

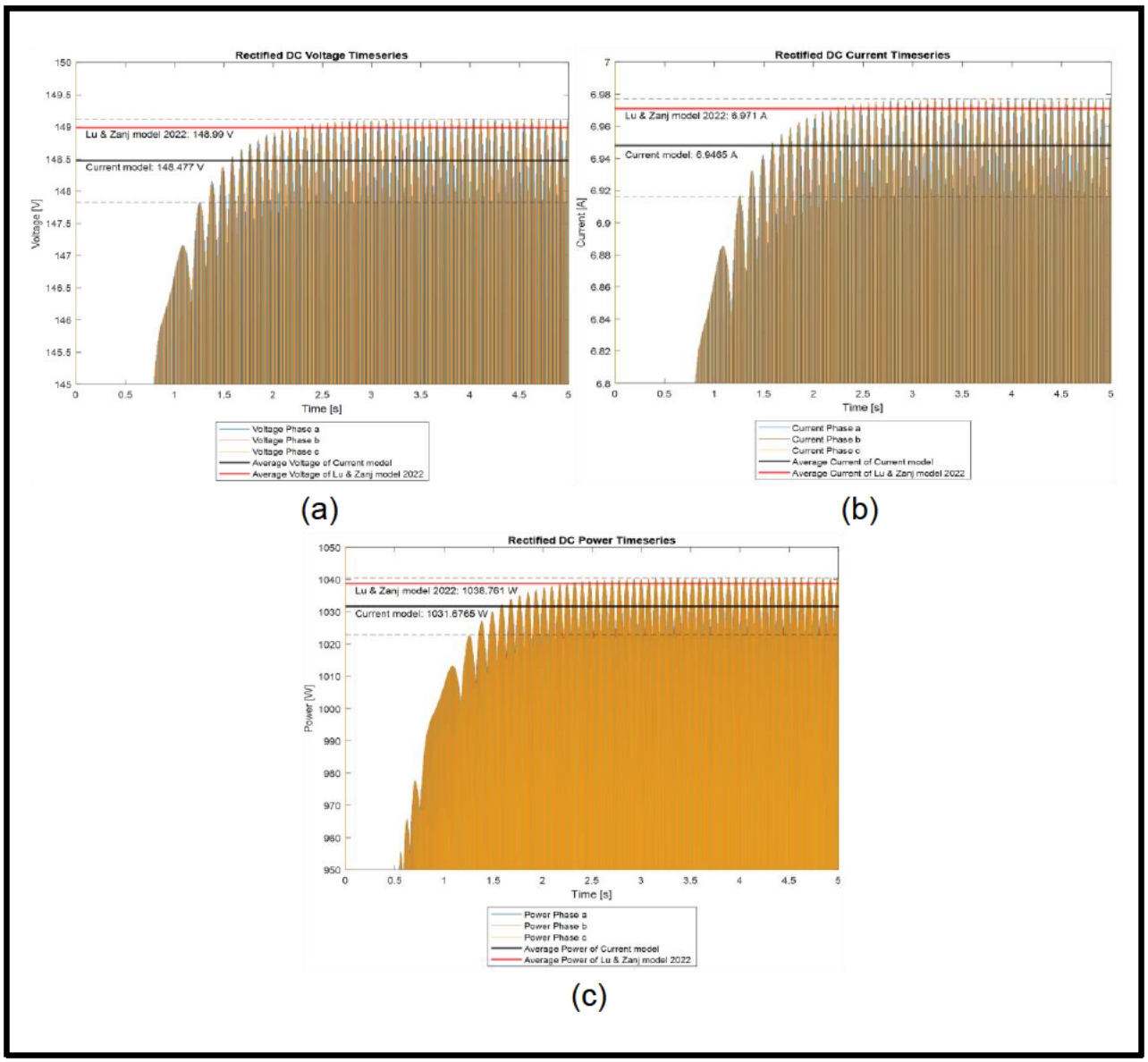

Figure 25 DC electrical outputs derived from three-phase electrical outputs (a) DC Voltage; (b) DC Current; (c) DC Power

simulation for 2 seconds as seen in Figure 25. The average voltage, current, and power of the results from current model are 148.477 V, 6.9465 A, and 1031.6765 W, respectively. In comparison, the model proposed by Lu and Zanj yield slightly higher values of 148.99 V, 6.971 A, and 1038.761 W for voltage, current, and power, respectively. This can be explained that the state-space equations require both aerodynamic torque and angular velocity to determine electrical outputs. Therefore, increasing torque and velocity will result in higher electrical outputs.

Comparison on Experimental Setup

In this section, the focus is on the experimental results. The section will be divided into two parts. The first part will analyse the results of different fan setups to determine which is better. The second part will use the best setup to validate the mathematical model.

Comparison on Results of Two Fan Setups

Several tests have been done regarding the experimental testing procedure for 3-fan and 4-fan setup proposed in Figure 18. Experimental results have been collected and analysed in Microsoft Excel, and a MATLAB code for plotting these results is shown in Appendix E.

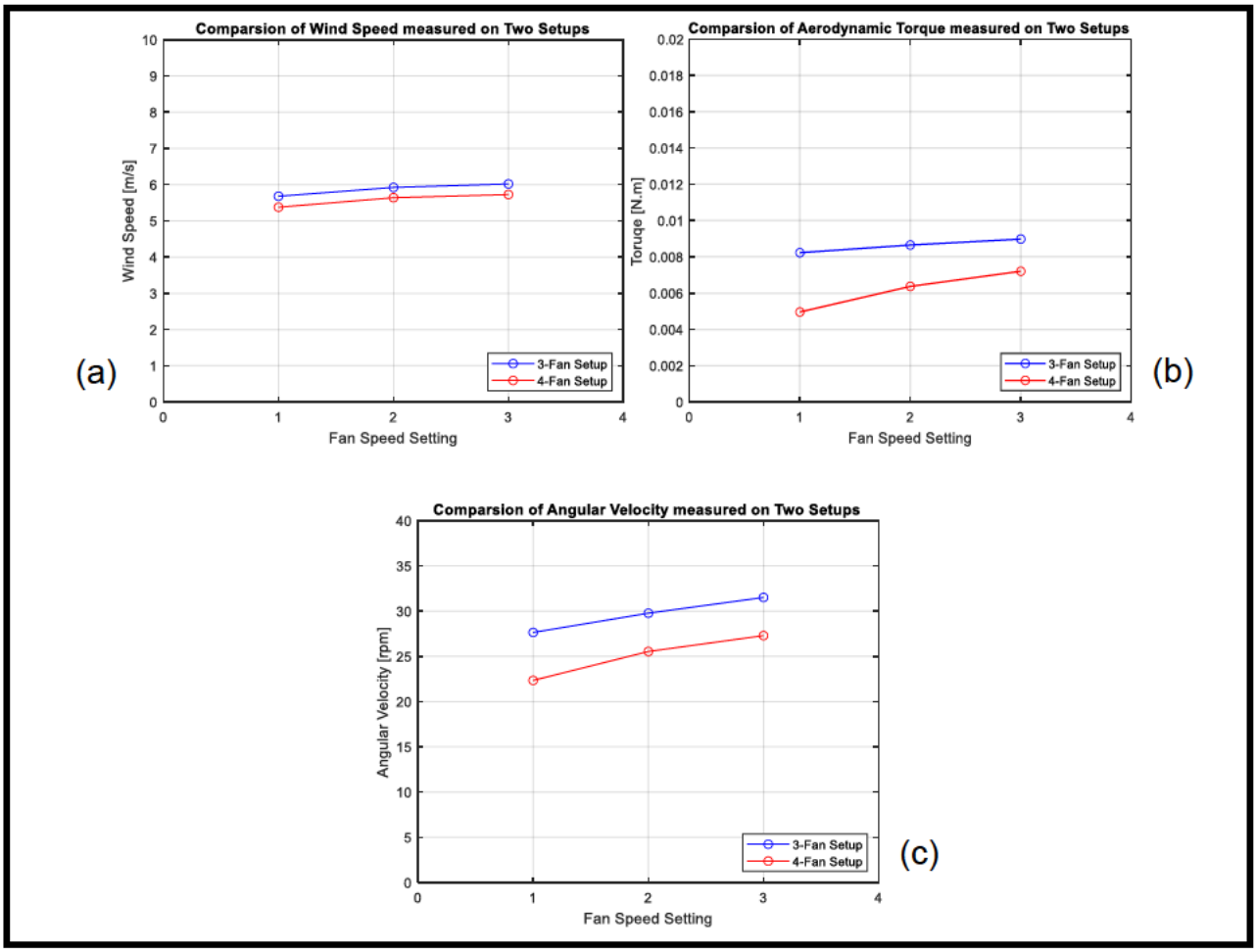

Figure 26 Experimental results of two setups on (a) Wind Speed; (b) Aerodynamic Torque; (c) Angular Velocity

According to the anemometer sensor data displayed in Figure 26a, the turbine can receive the maximum wind velocity at fan speed level 3. the configuration with three fans offers better quality of airflow compared to the configuration with four fans. Similar trends were observed in the aerodynamic torque and angular velocity data collected from the load cell and tachometer sensors, respectively. According to Figure 26b, the three-fan configuration produces the highest torque at fan speed level 3, reaching a maximum of 0.009 N.m. The configuration described previously resulted in a maximum angular velocity of 32 rpm, as shown in Figure 26c. Furthermore, the experimental electrical results collected from DC Electronic Load device presented in Appendix F demonstrate a similar pattern.

As a result, the results generated from three fans configuration will be used for validation against the mathematical model proposed in this study.

Experimental Setup and Mathematical Model Outputs Comparison

The information contained in Table 5 is based on the findings presented in Figure 26. Thus, the parameters listed in Table 5 and

Table 6 are then inserted into the MATLAB code provided in Appendix A to generate Cp, TSR and aerodynamic torque for validation. These outputs will be used in another MATLAB code in Appendix G to generate the results shown in Figure 27.

Table 5 Summarised experimental results collected three fans configuration

Fan Speed / Parameter	1	2	3
$V_\infty\ [m/s]$	5.6792	5.9218	6.0179
$\omega\ [rpm]$	27.644	29.771	31.511

Table 6 VAWT characteristics of VX-6/5 prototype for validation

Parameter	Value	Unit
R	0.3415	m
H	1	m
c	0.0816	m
N	2	
Ψ	180	degree
V_∞	Refer to Table 5	m/s
ω	Refer to Table 5	rpm

According to Figure 27a, the experimental aerodynamic torque is lower than the mathematical model results. However, the current mathematical model results are closer to the experimental results than the results from the Lu & Zanj (2022) study. At a wind velocity of 6.018 m/s, the VX-6/5 prototype is exerted a torque of 0.009 N.m. The current model and Lu and Zanj model are exerted torques of 0.01 N.m and 0.012 N.m, respectively. Furthermore, the result Cp vs TSR in current model is closer to the experimental result than the result of the Lu and Zanj model. Moreover, the Cp value is observed to increase as the TSR increases. However, this trend is not as prominent in the results of both mathematical models, as depicted in Figure 27b.

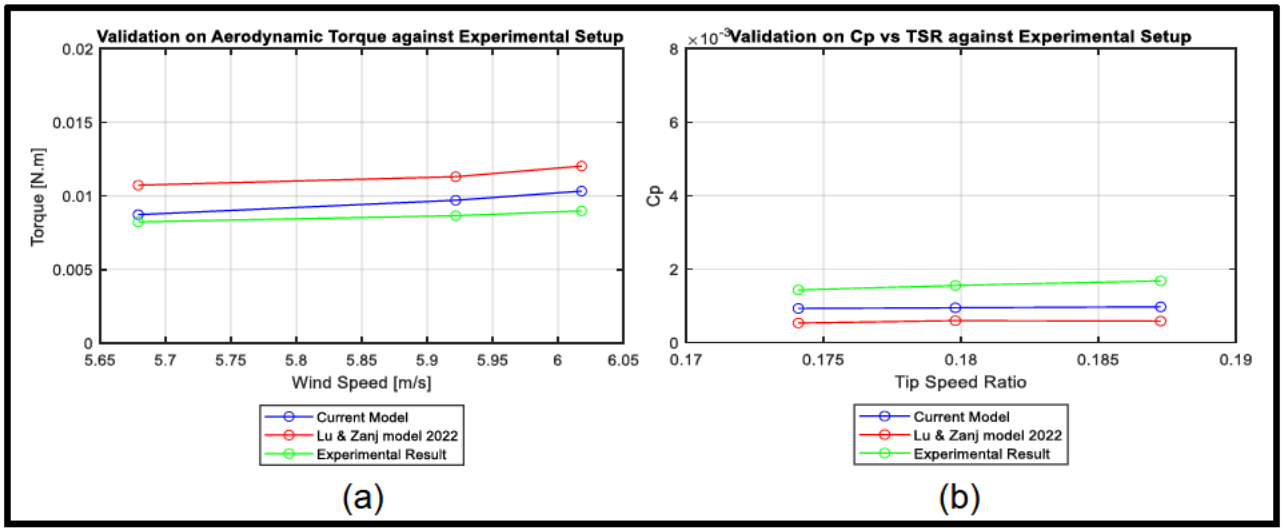

Figure 27 Validation of the mathematical model with experimental results collected from 3-fan setup (a) Aerodynamic Torque; (b) C_p vs TSR

Therefore, it is apparent that the findings obtained from the proposed Gorlov VAWT model have the potential to more accurately reflect the VX-6/5 outputs than the previous model introduced by Lu & Zanj (2022).

DISCUSSION

In the discussion section, it is critical to examine the results in relation to the project goals outlined earlier in this study. The main objective is to verify the new helical-blade VAWT model and integrate it into the current parametric model. Before this can be done, it is important to confirm the accuracy of the new model by comparing them with various VAWT models previously published. Additionally, the new model must be validated against the VX-6/5 prototype owned by VAWT-X Energy. The results presented in sections 'Comparison on Aerodynamic Model' and 'Comparison on Experimental Setup' will be discussed in conjunction, while the results presented in the 'Comparison on Parametric Model' section will be discussed separately.

Accuracy of the Gorlov VAWT

At the beginning of this study, it was challenging to differentiate between the proposed model in this study and the one introduced by Lu and Zanj (2022). Since all parametric VAWT models found in the literature applied very similar physical principles and theories. However, the coding algorithms used to implement these models can vary significantly. The most significant factor in distinguishing between the straight-bladed and helical-bladed vertical axis wind turbines is the result of torque distribution, as shown in Figure 20. In a helical-bladed VAWTs, the torque is distributed uniformly throughout the rotation of the turbine. This is not the case for straight-bladed VAWTs, where torque is at its highest at certain locations and very low or even negative at others. According to Figure 20, the torque decreases when the airfoil is parallel to the airflow, which occurs at locations near -90˚ and 90˚. the AOA is extremely minimal and even reaches zero in these sections, leading to low and even negative torque exerted on the blades in these areas. One way to address this phenomenon is to replace with helical blade. This unique shape of blade enables the turbine to face the airflow from any directions. This statement affirms the findings of Moghimi and Motawej (2020a), which suggested that the use of helical blades can decrease the torque instability that is often observed in straight-blade VAWTs.

Moreover, the proposed model has demonstrated to have strong agreements in results while comparing with different VAWT models in the literature. The following Table 7 contains a summary of results collected from Figure 19, Figure 21 and Figure 22.

Table 7 General comments on validation of proposed aerodynamic model

	VAWT in Lu and Zanj (2022)	VAWT in Moghimi and Motawej (2020)	VAWT in Paraschivoiu (2009)
TSR operation range	1.3 to 8.2	0.7 to 6.5	1.3 to 9.8
Maximum C_p	0.59 at 4.5 TSR	0.49 at 3.6 TSR	0.48 at 5.6 TSR
C_p lower than 0.1	below 2.6 TSR, and above 8 TSR	below 2.5 TSR, and above 6.3 TSR	below 2.9, and above 9.4 TSR
Comments	• Big range of operation • High C_p, but unrealistic • Best range with C_p higher than 0.1	• Small range of operation • Can achieve good C_p at low TSR • Small range with C_p higher than 0.1	• Best range of operation • Good C_p achieved at high TSR • Big range with C_p higher than 0.1

From Table 7, It is clear that the two-bladed VAWT (Lu & Zanj 2022; Paraschivoiu 2009) has the better TSR operation range then the three-bladed VAWT introduced in Moghimi and Motawej (2020). Furthermore, it can be observed that the range with a C_p greater than 0.1 is larger in the case of a two-bladed VAWT compared to a three-bladed one. However, in order to achieve the maximum power coefficient C_p, a higher TSR was necessary for two-bladed VAWT. Besides of those findings, the validity of the proposed model was demonstrated as the results generated closely matched the results of three other studies examined in this research.

Apart from that, the experimental setup also plays an important role in confirming on the accuracy of the proposed model. It was not initially anticipated that the results would show better performance for the three fan configurations. Prior to this study, the VX-6/5 had always been tested using a four-fan configuration. The discovery is significant as it assists in identifying the optimal setup for validating the mathematical model. Furthermore, the enhancement of the VX-6/5 model is demonstrated to be essential for the restoration of the experimental testing. With aid of the wind tunnel, the experimental setup is able to rotate at maximum speed of 60 rpm in the absence of any electrical load. Therefore, the experimental results was successfully collected and analysed against the mathematical model results. These results again demonstrate the accuracy of the proposed model, as they closely match the results of the physical testing prototype.

Connectivity between Gorlov VAWT model and Generator model

As discussed in the Case Study section, the parametric model owned by VAWT-X Energy consists of aerodynamic model and generator model. Even though the new aerodynamic model has found to be accurate by comparing with other results in the literature, it is still important for it to be integrated with the generator model to become the complete system. When comparing the results of the new parametric model with those of the existing parametric model (Lu and Zanj 2022), the input parameters were kept the same as stated in that study. The rotational speed of 260 rpm used in this comparison was also taken from the paper that was cited. In the previous discussion section, it is evident that the results of C_p are heavily influenced by the initial angular velocity input into the model. According to VAWT characteristics in Lu and Zanj paper, the initial angular velocity was set to 260 rpm, resulting in a 0.59 coefficient of performance that was very close to the Betz limit. While two other studies showed a lower angular velocity of 125 rpm, which resulted in a much lower C_p of approximately 0.49. Although the results of this comparison indicate that two models are in strong agreement, the aerodynamic results are still not realistic in terms of power coefficient. Nevertheless, the main goal for this activity is to determine how the new proposed aerodynamic model is connected to the current generator model. Hence, enhancing the overall performance of a parametric model or the specific performance of a general model is not within the scope of this study.

Limitations and Suggestions on Future Work

Limitations	Suggestions on Future Work
The proposed Gorlov VAWT model can simulate the aerodynamic results more accurately than the existing aerodynamic model. However, it is not operational at low speed (less than 3.5 m/s) due to the complexity of the aerodynamic equations, which causes negative values during calculations that have not yet been resolved.	One way to enhance the performance of the Gorlov VAWT model is to improve the upstream and downstream functions that were designed for straight-bladed turbines. These functions may not fully account for the added complexity of the helical shape. Moreover, the coding algorithms could be modified to perform the upstream and downstream calculations can be performed for each stream tube simultaneously instead of carrying out the upstream calculations first and the downstream calculations afterwards.
The proposed model has proven to be integrated well with the generator model. The parametric model can imitate the performance and electrical outputs of a VAWT by using an aerodynamic model and generator model. Nonetheless, there are still components that can be integrated into this model, such as the Eddy Current Brake, which requires more expertise in electromagnetism.	Every turbine requires an effective braking system to endure harsh wind conditions. Therefore, Eddy Current Brake is essential for VAWT-X Wind Turbines. Implementing this can significantly increase the controllability of turbine. Additionally, the capacity of the model can be enhanced by refining the state-space equations and the parametric model in MATLAB/Simulink.
The self-start issue with the VX-6/5 prototype has been resolved. However, the turbine is only rotating at a slow speed, which is around 60 rpm, without an electrical load. The reason for this could be that the fan output is low, the VX-6/5 is far away from the wind source, or the wind tunnel structure is incomplete.	By upgrading the wind generation source, such as replacing with more powerful fans or adding more fans at the other end of wind tunnel, might improve the wind power. Furthermore, the wind quality may be improved by installing a honeycomb structure in the wind tunnel and moving the VX-6/5 prototype closer to the source of wind.

CONCLUSION

The primary aim of the study is to optimise and increase the capacity of the existing mathematical model and experimental setup of VAWT-X wind turbines. To do that, several goals and objectives must be met. The study involved creating a new model of the helical-blade Gorlov VAWT and implementing it in MATLAB. The model took into account the effect of helical angles on the blades. Additionally, modifications were made to the VX-6/5 prototype to increase its testing capacity and address the self-starting issue. Afterwards, the wind tunnel should be built in order to improve the wind conditions for experimental tests. Furthermore, it is crucial to validate the accuracy of the proposed new aerodynamic model and effectively integrate it with the existing generator model. This has been achieved through comparing the results of aerodynamic model with various VAWT models present in the literature, as well as experimental data collected from VX-6/5 prototype. In addition, the strong agreement on the results of the proposed parametric model with the existing parametric model demonstrates that it can be effectively integrated with the generator model. Moreover, the torque distribution results show a significant difference in torque exerting on blades between straight-bladed and helical-bladed VAWTs.

Discussion of limitations and proposed suggestions for future work are provided. To solve the problem of not being able to function at wind speeds below 3.5 m/s, improvements need to be made in the upstream and downstream functions, as well as in the coding algorithms. In addition, refining the state-space equations in the generator model and adding Eddy Current Brake system can further increase the capacity and controllability of the model. Moreover, the experimental setup can be further improved by replacing more power fans, adding more fans at the other end of the wind tunnel, installing a honeycomb structure to the wind tunnel and moving VX-6/5 closer to the wind source, are can potentially increase the wind quality and testing capacity of the experimental setup.

The successful of this study will be beneficial for the development of VAWT-X Energy technologies. It is hoped that this research will contribute into addressing the lack of knowledge and research in helical-blade VAWT technology.

BIBLIOGRAPHY

Adams, Z & Chen, J 2017, 'Flux-Line Theory: A Novel Analytical Model for Cycloturbines', *AIAA Journal*, vol. 55, no. 11, pp. 3851-3867, viewed 13 February 2023, DOI:/10.2514/1.J055804.

AirfoilTools n.d., *NACA 0015 (naca0015-il)*, AirfoilTools, viewed 12 March 2023, <http://airfoiltools.com/airfoil/details?airfoil=naca0015-il>.

Alaimo, A, Esposito, A, Messineo, A, Orlando, C & Tumino, D 2015, '3D CFD Analysis of a Vertical Axis Wind Turbine', *Energies*, vol. 8, no. 4, pp. 3013-3033, viewed 16 February 2023, DOI:/10.3390/en8043013.

Bai, C J & Wang, W C 2016, 'Review of computational and experimental approaches to analysis of aerodynamic performance in horizontal axis wind turbines (HAWTs)', *Renewable and Sustainable Energy Reviews*, vol. 63, pp. 506-519, viewed 9 February 2023, DOI:/10.1016/j.rser.2016.05.078.

Beri, H & Yao, Y 2011a, 'Numerical Simulation of Unsteady Flow to Show Self-starting of Vertical Axis Wind Turbine Using Fluent', *Journal of Applied Sciences*, vol. 11, no. 6, pp. 962-970, viewed 12 February 2023, DOI:/10.3923/jas.2011.962.970.

Beri, H & Yao, Y 2011b, 'Double Multiple Stream Tube Model and Numerical Analysis of Vertical Axis Wind Turbine', *Energy and Power Engineering*, vol. 3, pp. 262-270, viewed 8 March 2023, DOI:/10.4236/epe.2011.33033.

Bertram, V 2012, *Practical Ship Hydrodynamics*, 2nd ed, Butterworth-Heinemann, Amsterdam.

Burton, T, Jenkins, N, Sharpe, D & Bossanyi, E 2011, *Wind Energy Handbook*, Wiley, USA.

Castelli, M R, Simioni, G & Benini, E 2012, 'Numerical analysis of the influence of airfoil asymmetry on VAWT performance', *International Journal of Aerospace and Mechanical Engineering*, vol. 61, no. 1, viewed 12 February 2023, DOI:/10.5281/zenodo.1332788.

Chen, J, Chen, L, Xu, H, Yang, H, Ye, C & Liu, D 2016, 'Performance improvement of a vertical axis wind turbine by comprehensive assessment of an airfoil family', *Energy*, vol. 114, pp. 318-331, viewed 12 February 2023, DOI:/10.1016/j.energy.2016.08.005.

Cheng, Q, Liu, X, Ji, H S, Kim, K C & Yang, B 2017, 'Aerodynamic Analysis of a Helical Vertical Axis Wind Turbine', *Energies*, vol. 10, no. 4, pp. 575, viewed 17 February 2023, DOI:/10.3390/en10040575.

Dixon, K R 2008, 'The near wake structure of a vertical axis wind turbine', Master thesis, Delft University of Technology, Netherlands.

Drzewiecki, S 1920, *Théorie Générale de L'Hélice*, University of Michigan Library, French.

Ebrahimpour, M, Shafaghat, R, Alamian, R & Shadloo, M S 2019, 'Numerical Investigation of the Savonius Vertical Axis Wind Turbine and Evaluation of the Effect of the Overlap Parameter in Both Horizontal and Vertical Directions on Its Performance', *Symmetry*, vol. 11, no. 6, pp. 821, viewed 10 February 2023, DOI:/10.3390/sym11060821.

Edenhofer, O 2014, *Climate change 2014 : mitigation of climate change : Working Group III contribution to the Fifth assessment report of the Intergovernmental Panel on Climate Change*, ed. Edenhofer, O, Cambridge University Press, Cambridge, England.

Energy.gov.au 2022, *Renewables*, Energy.gov.au, Australia, viewed 8 February 2023, < https://www.energy.gov.au/data/renewables>.

Engineering Toolbox 2003a, *Air - Dynamic and Kinematic Viscosity*, Engineering Toolbox, viewed 20 March 2023, <https://www.engineeringtoolbox.com/air-absolute-kinematic-viscosity-d_601.html>.

Engineering Toolbox 2003b, *Air - Density, Specific Weight and Thermal Expansion Coefficient vs. Temperature and Pressure*, viewed 20 March 2023, <https://www.engineeringtoolbox.com/air-density-specific-weight-d_600.html>.

Francis, J 2022, 'Vertical Axis Wind Turbine Control System Design', Honours thesis, Flinders University, Adelaide, Australia.

Froude, W 1920, 'On the elementary relation between pitch, slip, and propulsive efficiency', United States Government, accessed 10 February 2023.

Gato, L M C & Falcao, A 1988, 'Aerodynamics of the Wells turbine', *International Journal of Mechanical Sciences*, vol. 33, no. 6, pp. 283-395, viewed 13 February 2023, DOI:/10.1016/0020-7403(88)90012-4.

Gato, L M C & Falcao, A 1990, 'Performance of the Wells turbine with double row of guide vanes', *JSME International Journal*, vol. 33, no. 2, pp. 265-271, viewed 13 February 2023, DOI:/10.1299/jsmeb1988.33.2_265.

Gato, L M C & Falcao, A 2012, 'Air Turbines', *Comprehensive Renewable Energy*, Elsevier, Amsterdam, pp. 111-149.

Glauert, H 1935, 'Windmills and fans', in W Durand (ed.), *Aerodynamic Theory*, Springer, New York, pp. 324-340.

Global Wind Energy Council 2015, *Global Wind Report 2015*, Global Wind Energy Council, Belgian Government, accessed 8 February 2023.

Gorlov, A M 1995, *Unidirectional helical reaction turbine operable under reversible fluid flow for power systems*, 5451137.

Gudmundsson, S 2014, 'Chapter 14 - The Anatomy of the Propeller', *General Aviation Aircraft Design - Applied Methods and Procedures*, Saint Louis: Elsevier.

Gudmundsson, S 2014, *General Aviation Aircraft Design*, Butterworth-Heinemann, UK, doi: 10.1016/B978-0-12-397308-5.00014-3.

Hashem, I & Mohamed, M H 2017, 'Aerodynamic performance enhancements of H-rotor Darrieus wind turbine', *Energy*, vol. 142, pp. 531-545, viewed 13 March 2023, DOI:/10.1016/j.energy.2017.10.036.

Hawthorne, W R & Horlock, J H 1964, 'Actuator Disc Theory of the Incompressible Flow in Axial Compressors', *Proceedings of the Institution of Mechanical Engineers*, vol. 174, no. 1, pp. 789-814, viewed 13 February 2023, DOI:/10.1243/PIME_PROC_1962_176_063_02.

IEA 2021, *Pathway to critical and formidable goal of net-zero emissions by 2050 is narrow but brings huge benefits, according to IEA special report*, IEA, viewed 8 February 2023, < https://www.iea.org/news/pathway-to-critical-and-formidable-goal-of-net-zero-emissions-by-2050-is-narrow-but-brings-huge-benefits>.

IPCC 2022, ‘Climate Change 2022: Mitigation of Climate Change’, IPCC, Swiss Government, accessed 6 February 2023.

Islam, M, Ting, D S -K & Fartaj, A 2008, ‘Aerodynamic models for Darrieus-type straight-bladed vertical axis wind turbines’, *Renewable and Sustainable Energy Reviews*, vol. 12, no. 4, pp. 1087-1109, viewed 10 February 2023, DOI:/10.1016/j.rser.2006.10.023.

Jafari, M, Razavi, A & Mirhosseini, M 2018, ‘Effect of airfoil profile on aerodynamic performance and economic assessment of H-rotor vertical axis wind turbines’, *Energy*, vol. 165, pp. 792-810, viewed 13 March 2023, DOI:/10.1016/j.energy.2018.09.124.

Jiang, Y, Zhao, P, Stoesser, T, Wang, K & Zou, L 2020, ‘Experimental and numerical investigation of twin vertical axis wind turbines with a deflector’, *Energy Conversion and Management*, vol. 209, pp. 112588, viewed 9 February 2023, DOI:/10.1016/j.enconman.2020.112588.

Kanyako, F & Janajreh, I 2014, ‘Vertical Axis Wind Turbine performance prediction for low wind speed environment’, *2014 IEEE Innovations in Technology Conference*, USA, 16 May.

Katz, J & Plotkin, A 2012, *Low-speed Aerodynamics*, 2nd ed, Cambridge University Press, England.

Lakshminarayana, B 1996, *Fluid Dynamics and Heat Transfer of Turbomachinery*, Wiley, New York.

Lu, B & Zanj, A 2022, ‘Development of an integrated system design tool for helical Vertical Axis Wind Turbines (VAWT-X)’, *Energy Reports*, vol. 8, pp. 8499-8510, viewed 9 August 2022, DOI:/10.1016/j.egyr.2022.06.038.

Lu, B 2021, ‘Modelling and Performance Analysis of a VAWT-X Wind Turbine for Parametric Design’, Honours thesis, Adelaide, Australia.

McLaren, K W 2011, ‘A Numerical and Experimental Study of Unsteady Loading of High Solidity Vertical Axis Wind Turbines’, PhD Thesis, McMaster University, Canada.

Meana-Fernández, A, Solís-Gallego, I, Fernández Oro, J M, Argüelles Díaz, K M & Velarde-Suárez, S 2018, 'Parametrical evaluation of the aerodynamic performance of vertical axis wind turbines for the proposal of optimized designs', *Energy*, vol. 147, pp. 504-517, viewed 11 March 2023, DOI:/10.1016/j.energy.2018.01.062.

Migliore, P & Fritschen, J 1982, 'Darrieus wind-turbine airfoil configurations', United States Government, accessed 10 February 2023.

Moghimi, M & Motawej, H 2020a, 'Developed DMST model for performance analysis and parametric evaluation of Gorlov vertical axis wind turbines', *Sustainable Energy Technologies and Assessments*, vol. 37, pp. 100616, viewed 10 November 2022, DOI:/10.1016/j.seta.2019.100616.

Moghimi, M & Motawej, H 2020b, 'Investigation of Effective Parameters on Gorlov Vertical Axis Wind Turbine', *Fluid Dynamics*, vol. 55, pp. 345-363, viewed 11 November 2022, DOI:/10.1134/S0015462820030106.

Nikam, D A & Kherde, S M 2015, 'Literature review on design and development of vertical axis wind turbine blade', *International Journal of Engineering Research and Applications*, pp. 156-161.

Niranjana, S J 2015, 'Power Generation by Vertical Axis Wind Turbine', *Emerging Research in Management &Technology*, vol. 4, no. 7.

Paraschivoiu, I 1981, 'Double–multiple stream tube model for Darrieus wind turbine', *NASA. Lewis Research Center Wind Turbine Dyn*, USA, 1 May.

Paraschivoiu, I 1982, 'Aerodynamic Loads and Performance of the Darrieus Rotor', *Journal of Energy*, vol. 6, no. 6, pp. 406-412, viewed 18 November 2022, DOI:/10.2514/3.62621.

Paraschivoiu, I 1983, 'Double multiple streamtube model with recent improvements', *Journal of Energy*, vol. 7, no. 3, pp. 250-255, viewed 20 November 2022, DOI:/10.2514/3.48077.

Paraschivoiu, I 2002, *Wind turbine design: with emphasis on Darrieus concept*, Presses internationales Polytechnique, USA.

Paraschivoiu, I 2009, ‘H-Darrieus Wind Turbine with Blade Pitch Control’, *International Journal of Rotating Machinery*, viewed 20 December 2022, DOI:/10.1155/2009/505343.

Princeton University n.d., *Streamlines and Streamtubes*, Princeton University, United States, viewed 10 February 2023, <https://www.princeton.edu/~asmits/Bicycle_web/streamline.html#:~:text=These%20streamlines%20form%20a%20tube,tube%20is%20called%20a%20streamtube>.

Saeidi, D, Sedaghat, A, Alamdari, P & Alemrajabi, A A 2013, ‘Aerodynamic design and economical evaluation of site specific small vertical axis wind turbines’, *Applied Energy*, vol. 101, pp. 765-775, viewed 9 March 2023, DOI:/10.1016/j.apenergy.2012.07.047.

Scheurich, F, Fletcher, T M & Brown, R E 2010, ‘The influence of blade curvature and helical blade twist on the performance of a vertical-axis wind turbine’, *2010 Aerospace Sciences Meeting*, Orlando, Florida, 4-7 January.

Sharpe, T & Proven, G 2010, ‘Crossflex: concept and early development of a true building integrated wind turbine’, *Energy and Buildings*, vol. 42, no. 12, pp. 2365-2375, viewed 10 February 2023, DOI:/10.1016/j.enbuild.2010.07.032.

Solomin, E, Lingjie, X, Jia, H & Danping, D 2020, ‘Comprehensive Comparison of the Most Effective Wind Turbines’, *Advances in Automation*, Springer Cham.

Somers, D M, Maughmer, M D 2003, ‘Theoretical Aerodynamic Analyses of Six Airfoils for Use on Small Wind Turbines: July 11, 2002--October 31, 2002’, United States Government, accessed 10 February 2023.

Stepniewski, W Z 1984, ‘Rotary-wing aerodynamics’, United States Government, accessed 10 February 2023.

Strickland, J H, Webster, B T & Nguyen, T 1979, ‘A Vortex Model of the Darrieus Turbine: An Analytical and Experimental Study’, *Journal of Fluids Engineering*, vol. 101, no. 4, pp. 500-505, viewed 16 February 2023, DOI:/10.1115/1.3449018.

Subramanian, A, Yogesh, S A, Sivanandan, H, Giri, A, Vasudevan, M, Mugundhan, V & Velamati, R K 2017, ‘Effect of airfoil and solidity on performance of small scale vertical

axis wind turbine using three dimensional CFD model', *Energy*, vol. 133, pp. 179-190, viewed 12 February 2023, DOI:/10.1016/j.energy.2017.05.118.

Sun, X & Zhou, D 2022, 'Review of Numerical and Experimental Studies on Flow Characteristics around A Straight-bladed Vertical Axis Wind Turbine and Its Performance Enhancement Strategies', *Archives of Computational Methods in Engineering*, vol. 29, no. 3, pp. 1839-1874, viewed 10 February 2023, DOI:/10.1007/s11831-021-09640-4.

Svorcan, J, Stupar, S, Komarov, D, Pekovic, O & Kostic, I 2013, 'Aerodynamic design and analysis of a small-scale vertical axis wind turbine', *Journal of Mechanical Science and Technology*, vol. 27, pp. 2367-2373, viewed 15 March 2023, DOI:/10.1007/s12206-013-0621-x.

Templin, R J 1974, 'Aerodynamic performance theory for the NRC vertical-axis wind turbine', National Aeronautical Establishment, Canadian Government, accessed 10 February 2023.

VAWT-X Energy 2022, *Products*,VAWT-X Energy, Australia, viewed 6 February 2023, <https://vawt-x.com.au/products/>.

Wang, L B, Zhang, L & Zeng, N D 2007, 'A potential flow 2-D vortex panel model: Applications to vertical axis straight blade tidal turbine', *Energy Conversion and Management*, vol. 48, no. 2, pp. 454-461, viewed 11 February 2023, DOI:/10.1016/j.enconman.2006.06.017.

Wang, X, Ye, Z, Kang, S & Hu, H 2019, 'Investigations on the unsteady aerodynamic characteristics of a horizontal-axis wind turbine during dynamic yaw processes', *Energies,* vol. 12, no. 16, pp. 3125, viewed 10 February 2023, DOI:/10.3390/en12163124.

Wang, Y F & Zhan, M S 2013, '3-Dimensional CFD simulation and analysis on performance of a micro-wind turbine resembling lotus in shape', *Energy and Buildings*, vol. 65, pp. 66-74, viewed 12 February 2023, DOI:/10.1016/j.enbuild.2013.05.045.

Wilson, R & Lissaman, P 1974, 'Applied Aerodynamics of Wind Power Machines', Oregon State University, United States Government, accessed 10 February 2023.

Zervos, A 1988, ‘Aerodynamic evaluation of blade profile for vertical axis wind turbines’, *European wind energy conference*, Herning, Denmark.

Zhao, Z, Qiang, S, Shen, W, Wang, T, Xu, B, Zheng, Y & Wang, R 2017, ‘Study on variable pitch strategy in H-type wind turbine considering effect of small angle of attack’, *Journal of Renewable and Sustainable Energy*, vol. 9, no. 5, pp. 053302, viewed 12 March 2023, DOI:/10.1063/1.4989795.

APPENDICES

Appendix A: MATLAB code Gorlov VAWT modelling on VX-6 and VX-6/5

Removed due to copyright restriction

Removed due to copyright restriction

Removed due to copyright restriction

Removed due to copyright restriction

Appendix B: MATLAB code for Comparison on Aerodynamic Model

Removed due to copyright restriction

Appendix C: MATLAB/Simulink code of Generator model

1) State-space equations and state variables in generator model

The following series of equations describe the state-space equation in the generator model (Lu and Zanj 2022).

$$\frac{d}{dt}\begin{bmatrix} x_1 \\ x_2 \\ x_3 \\ x_4 \\ x_5 \\ x_6 \\ x_7 \end{bmatrix} = \begin{bmatrix} -\frac{b}{J}x_1 - \frac{\psi}{L}\left(x_3 \sin\left(n_p x_2\right) + x_5 \sin\left(n_p x_2 + \frac{2\pi}{3}\right) + x_7 \sin\left(n_p x_2 + \frac{4\pi}{3}\right)\right) \\ \frac{x_1}{J} \\ -\frac{\psi n_p}{J} \cdot x_1 \cdot \sin\left(n_p x_2\right) - \frac{R_a}{L}x_3 \\ \frac{x_1}{J} \\ -\frac{\psi n_p}{J} \cdot x_1 \cdot \sin\left(n_p x_4 + \frac{2\pi}{3}\right) - \frac{R_b}{L}x_5 \\ \frac{x_1}{J} \\ -\frac{\psi n_p}{J} \cdot x_1 \cdot \sin\left(n_p x_6 + \frac{4\pi}{3}\right) - \frac{R_b}{L}x_7 \end{bmatrix} + \begin{bmatrix} u_1 + \tau_{ECB}\left(u_2\right) \\ 0 \\ 0 \\ 0 \\ 0 \\ 0 \\ 0 \end{bmatrix}$$

The following equation describes the matrix of variables by applying integration to the state-space equations in the generator model (Lu and Zanj 2022).

$$x = [p \quad \theta_a \quad \lambda_a \quad \theta_b \quad \lambda_b \quad \theta_c \quad \lambda_c]$$

2) VX-6 parameters used in parametric model comparison

The following table presents all parameters used in the MATLAB/Simulink code, including all geometrical parameters of turbine, and electrical parameters of generator model.

Parameter	Value	Unit
L_r	0.036	[H]
ψ	0.8419	[Wb]
J_{rotor}	3.2714	[m^4]
b	11.8	[kg/s]
n_p	12	[pole pairs]
r_r	0	[Ω]
r_{load}	21.3725	[Ω]
N	2	[1]
c	0.1875	[m]
H	5	[m]
R	1.5	[m]
Tuned parameter: b	8.8381	[kg/s]
Tuned system input: V_∞	11.2	[m/s]
Initial condition: x_1 (0)	89.0704	[kg m/s]

3) MATLAB code for generator model used in MATLAB/Simulink

The following code has been written in MATLAB/Simulink and used for integration with the aerodynamic model of Gorlov VAWT (Lu and Zanj 2022).

Removed due to copyright restriction

Appendix D: Three-phase Electrical Outputs of current parametric model

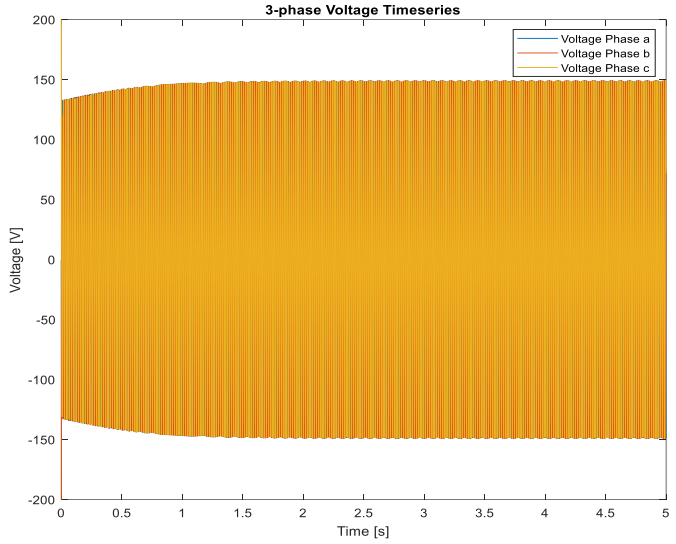

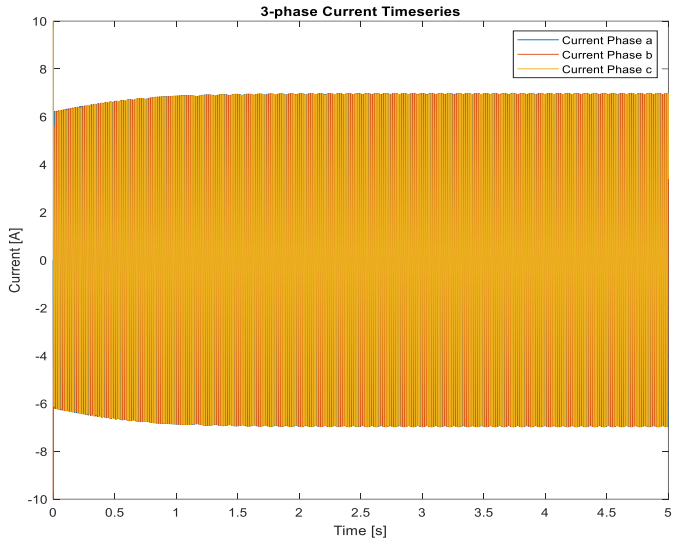

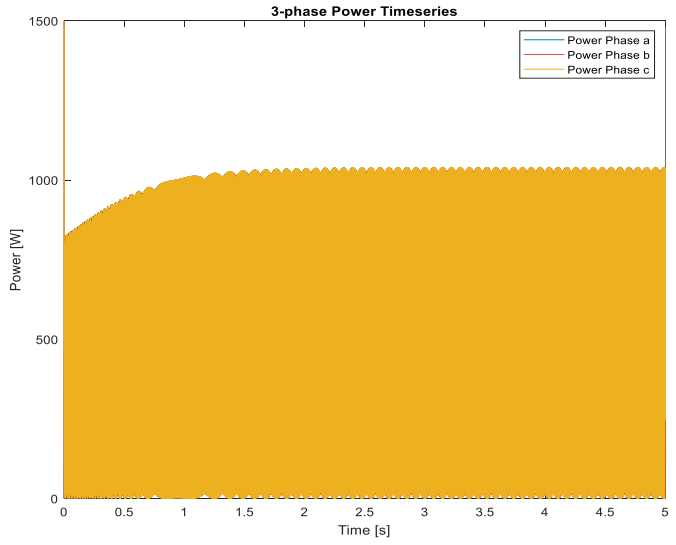

Appendix E: MATLAB code for Comparison on 3 fan speed settings

Removed due to copyright restriction

Removed due to copyright restriction

Appendix F: Experimental Electrical Outputs of VX-6/5 prototype collected from DC Electrical Load device

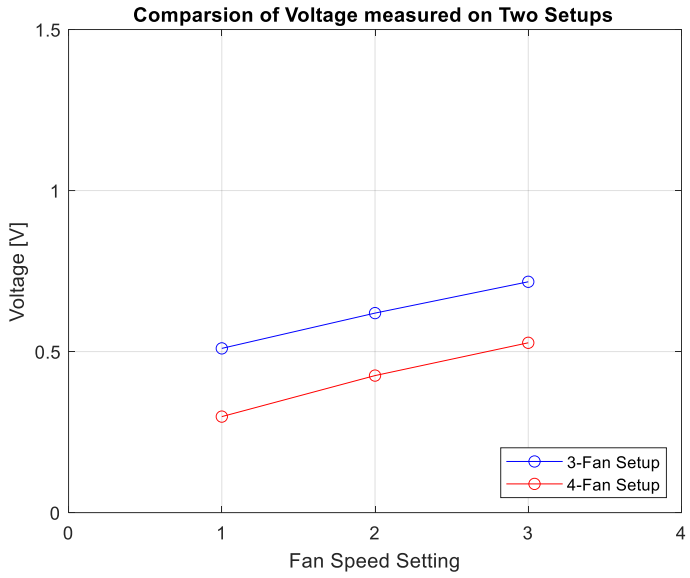

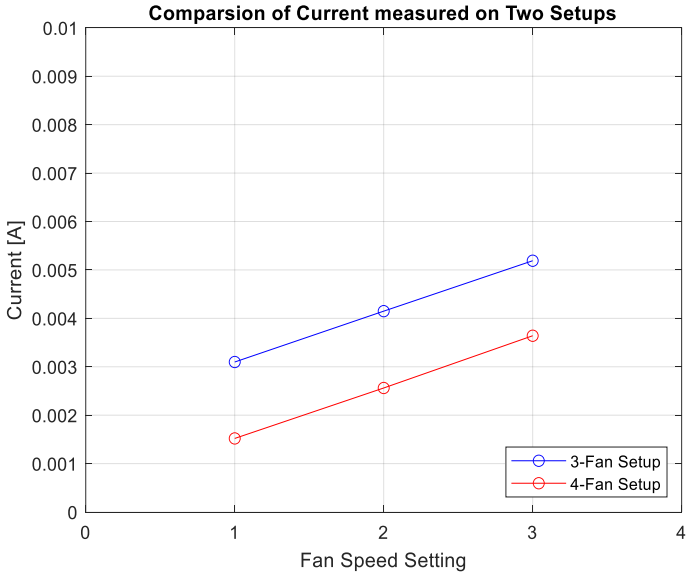

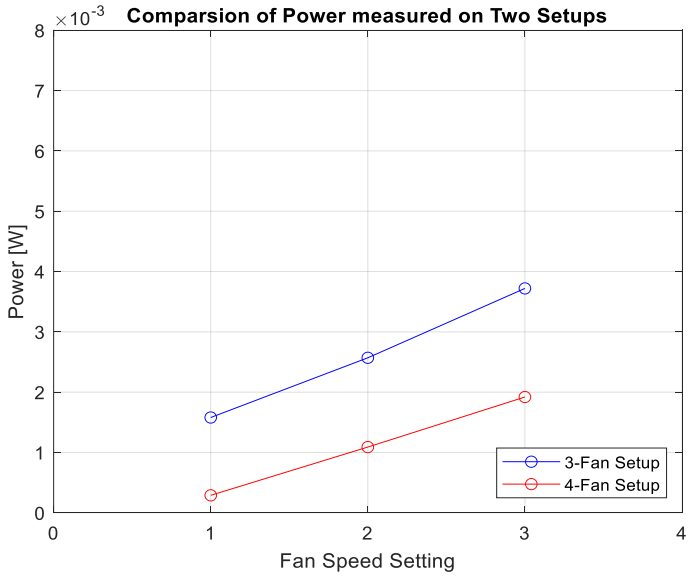

Appendix G: MATLAB code for Comparison on Experimental Setup

Removed due to copyright restriction